SIAM J. NUMER. ANAL.
Vol. 50, No. 5, pp. 2588–2611

OPTIMIZED SCHWARZ WAVEFORM RELAXATION AND DISCONTINUOUS GALERKIN TIME STEPPING FOR HETEROGENEOUS PROBLEMS*

LAURENCE HALPERN†, CAROLINE JAPHET‡, AND JÉRÉMIE SZEFTEL§

Abstract. We design and analyze a Schwarz waveform relaxation algorithm for domain decomposition of advection-diffusion-reaction problems with strong heterogeneities. The interfaces are curved, and we use optimized Ventcell transmission conditions. We analyze the semidiscretization in time with discontinuous Galerkin as well. We also show two-dimensional numerical results using generalized mortar finite elements in space.

Key words. coupling heterogeneous problems, optimized Schwarz waveform relaxation, time discontinuous Galerkin, nonconforming grids

AMS subject classifications. 65M15, 65M50, 65M55

DOI. 10.1137/120865033

1. Introduction. In many fields of applications such as reactive transport, far field simulations of underground nuclear waste disposal or ocean-atmosphere coupling, models have to be coupled in different spatial zones, with very different space and time scales and possible complex geometries. For such problems with long time computations, a splitting of the time interval into windows is necessary, with the possibility of using robust and fast solvers in each time window, see [21].

The optimized Schwarz waveform relaxation (OSWR) method was introduced for linear parabolic and hyperbolic problems with constant coefficients in [3]. It was analyzed and extended to linear advection-reaction-diffusion problems with constant coefficients in [18]. The algorithm computes in the subdomains on the whole time interval, exchanging space-time boundary data through optimized transmission operators. The operators are of Robin or Ventcell type (see [7, 19]) with coefficients minimizing the convergence factor of the algorithm, extending the strategy developed in [13, 14]. The optimization problem was analyzed in [1, 4].

This method potentially applies to different space-time discretizations in subdomains, possibly nonconforming, and needs a very small number of iterations to converge. Numerical evidence of the performance of the method with variable smooth coefficients was given in [18]. An extension to discontinuous coefficients was introduced in [2, 5]. In [5], asymptotically optimized Robin transmission conditions were given in some particular cases.

The discontinuous Galerkin finite element method in time offers many advantages. Rigorous analysis can be made for any degree of accuracy and local time stepping,

*Received by the editors February 7, 2012; accepted for publication August 5, 2012; published electronically October 23, 2012. The research of the first two authors was partially supported by French ANR (COMMA) and Gdr MoMas.
http://www.siam.org/journals/sinum/50-5/86503.html
†Université Paris 13, LAGA, CNRS, UMR 7539, F-93430, Villetaneuse, France (halpern@math.univ-paris13.fr).
‡Université Paris 13, LAGA, CNRS, UMR 7539, F-93430, Villetaneuse, France, INRIA Paris-Rocquencourt, BP 105, 78153 Le Chesnay, France, and CSCAMM, University of Maryland College Park, MD 20742 USA 93430 (japhet@math.univ-paris13.fr).
§Département de Mathématiques et Applications, Ecole Normale Supérieure, 75230 Paris cedex 05, France (Jeremie.Szeftel@ens.fr).

and time steps can be adaptively controlled by a posteriori error analysis; see [15,24]. In a series of presentations in the regular domain decomposition meeting we presented the DG-OSWR method, using discontinuous Galerkin for the time discretization of the OSWR. In [2,9], we introduced the algorithm in one dimension with discontinuous coefficients. In [11], we extended the method to the bidimensional case. For the space discretization, we extended numerically the nonconforming approach in [6] to advection-diffusion problems and optimized order 2 transmission conditions to permit nonmatching grids in time and space on the boundary. The space-time projections between subdomains were done by an optimal projection algorithm without any additional grid, as in [6]. Simulations in two dimensions with continuous coefficients were presented. In [12] we extended the proof of convergence of the OSWR algorithm on the partial differential equation to nonoverlapping subdomains with curved interfaces. Only sketches of proofs were presented.

The present paper intends to give a full and self-contained account of the nonoverlapping method for the advection diffusion reaction equation with variable coefficients and Ventcell transmission conditions.

In section 2, we present the Ventcell algorithms at the continuous level in any dimension and give in detail the new proofs of convergence of the algorithm for nonoverlapping subdomains with curved interfaces.

Then in section 3, we semidiscretize in time with discontinuous Galerkin and prove the convergence of the algorithms for flat interfaces.

We present in section 4 numerical results. The purpose is to perform local grid refinement via the domain decomposition approach—not to use the method for massively parallel computations. We first present a simulation with piecewise smooth coefficients and a curved interface, with an application to porous media equation, to show the convergence properties and analyze the error. We finally include an application inspired from ocean-atmosphere coupling. We give both theoretical and numerical analyses of the computational time when using domain decomposition or a conforming space-time grid in the domain. We also compare the number of iterations with the "classical" domain decomposition using a small overlap and transmission through Dirichlet data.

The analysis of the fully discrete problem is under investigation and will be treated in a forthcoming paper.

Consider the advection-diffusion-reaction equation in $\mathbb{R}^N$,

$$\partial_t u + \nabla \cdot (\boldsymbol{b}u - \nu \nabla u) + cu = f \quad \text{in } \mathbb{R}^N \times (0,T), \tag{1.1}$$

with initial condition

$$u(0,x) = u_0(x), \quad x \in \mathbb{R}^N. \tag{1.2}$$

We consider a decomposition of $\mathbb{R}^N$ into nonoverlapping subdomains $\Omega_i, i \in \{1,\ldots,I\}$, as depicted in Figure 1.1. The interfaces $\Gamma_{i,j} = \overline{\Omega}_i \cap \overline{\Omega}_j$ are varieties of dimension $N-1$ and are supposed to be hyperplanes at infinity.

The advection and diffusion coefficients $\boldsymbol{b}$ and ν are in $W^{1,\infty}(\Omega_i)$ and c in $L^\infty(\Omega_i)$ for each i. The problem is parabolic in the sense that $\nu \geq \nu_0 > 0$ a.e. in $\mathbb{R}^N$. Therefore problem (1.1)–(1.2) is well-posed; i.e., if the initial value u_0 is in $H^1(\mathbb{R}^N)$, and the right-hand side f is in $L^2(0,T;L^2(\mathbb{R}^N))$, then there exists a unique solution u of (1.1)–(1.2) in $H^1(0,T;L^2(\mathbb{R}^N)) \cap L^\infty(0,T;H^1(\mathbb{R}^N))$ (see [16]).

Problem (1.1) is equivalent to solving I problems in subdomains Ω_i, with transmission conditions on the interface $\Gamma_{i,j}$ given by $[u]=0$, $[(\nu\nabla u - \boldsymbol{b}u)\cdot \boldsymbol{n}_i] = 0$, where

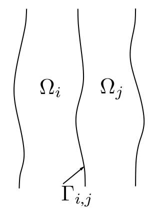

FIG. 1.1. *Decomposition in strips.*

$[v] := (v_i - v_j)|_{\Gamma_{i,j}}$ is the jump of v across $\Gamma_{i,j}$, and $\boldsymbol{n}_i$ is the unit exterior normal to Ω_i. Since the coefficients ν and $\boldsymbol{b}$ are possibly discontinuous on the interface, we note, for $s \in \Gamma_{i,j}$, $\nu_i(s) = \lim_{\varepsilon \to 0^+} \nu(s - \varepsilon \boldsymbol{n}_i)$. The same notation holds for $\boldsymbol{b}$ and c.

To any $i \in \{1, \dots, I\}$, we associate the set $\mathcal{N}_i$ of indices of the neighbors of Ω_i.

Following [2, 3, 5], we propose as preconditioner for (1.1)–(1.2) the sequence of problems

$$\partial_t u_i^k + \nabla \cdot (\boldsymbol{b}_i u_i^k - \nu_i \nabla u_i^k) + c_i u_i^k = f \text{ in } \Omega_i \times (0,T), \tag{1.3a}$$

$$\left(\nu_i \partial_{\boldsymbol{n}_i} - \boldsymbol{b}_i \cdot \boldsymbol{n}_i\right) u_i^k + \mathcal{S}_{i,j} u_i^k = \left(\nu_j \partial_{\boldsymbol{n}_i} - \boldsymbol{b}_j \cdot \boldsymbol{n}_i\right) u_j^{k-1} + \mathcal{S}_{i,j} u_j^{k-1} \text{ on } \Gamma_{i,j},\ j \in \mathcal{N}_i, \tag{1.3b}$$

defined via Ventcell boundary operators $\mathcal{S}_{i,j}$ acting on the part $\Gamma_{i,j}$ of the boundary of Ω_i shared by the boundary of Ω_j:

$$\mathcal{S}_{i,j}\varphi = p_{i,j}\varphi + q_{i,j}(\partial_t \varphi + \nabla_{\Gamma_{i,j}} \cdot (\boldsymbol{r}_{i,j}\varphi - s_{i,j} \nabla_{\Gamma i,j} \varphi)), \tag{1.4}$$

with respectively ∇_Γ and $\nabla_\Gamma \cdot$, the gradient and divergence operators on Γ. $p_{i,j}$, $q_{i,j}$, and $s_{i,j}$ are functions in $L^\infty(\Gamma_{i,j})$ and $\boldsymbol{r}_{i,j}$ is in $(L^\infty(\Gamma_{i,j}))^{N-1}$. The initial value is that of u_0 in each subdomain. An initial guess $(g_{i,j})$ is given on $L^2((0,T) \times \Gamma_{i,j})$ for $i \in \{1, \dots, I\}, j \in \mathcal{N}_i$. By convention for the first iterate, the right-hand side in (1.3b) is given by $g_{i,j}$. Under regularity assumptions, solving (1.1) is equivalent to solving (1.5)

$$\begin{aligned}
&\partial_t u_i + \nabla \cdot (\boldsymbol{b}_i u_i - \nu_i \nabla u_i) + c_i u_i = f \text{ in } \Omega_i \times (0,T),\\
&\left(\nu_i \partial_{\boldsymbol{n}_i} - \boldsymbol{b}_i \cdot \boldsymbol{n}_i\right) u_i + \mathcal{S}_{i,j} u_i = \left(\nu_j \partial_{\boldsymbol{n}_i} - \boldsymbol{b}_j \cdot \boldsymbol{n}_i\right) u_j + \mathcal{S}_{i,j} u_j \text{ on } \Gamma_{i,j} \times (0,T),\ j \in \mathcal{N}_i,
\end{aligned}$$

for $i \in \{1, \dots, I\}$ with u_i the restriction of u to Ω_i.

2. Studying the algorithm for the PDE.

The first step of the study is to give a frame for the definition of the iterates.

2.1. The local problem.

The optimized Schwarz waveform relaxation algorithm relies on the resolution of the following initial boundary value problem in a domain Ω, one of the Ω_i, with boundary Γ:

$$\begin{aligned}
&\partial_t w + \nabla \cdot (\boldsymbol{b} w - \nu \nabla w) + c w = f \text{ in } \Omega \times (0,T),\\
&\nu\, \partial_{\boldsymbol{n}} w - \boldsymbol{b} \cdot \boldsymbol{n}\, w + \mathcal{S} w = g \text{ on } \Gamma \times (0,T),\\
&w(\cdot, 0) = u_0 \text{ in } \Omega,
\end{aligned} \tag{2.1}$$

where $\boldsymbol{n}$ is the exterior unit normal to Ω, and $\mathcal{S}$ is the boundary operator defined on Γ by

$$\mathcal{S} w = p\, w + q\, (\partial_t w + \nabla_\Gamma \cdot (\boldsymbol{r} w - s \nabla_\Gamma w)). \tag{2.2}$$

The domain Ω is an infinite strip.

The functions p, q, and s are in $L^\infty(\Gamma)$, and $\boldsymbol{r}$ is in $(L^\infty(\Gamma))^{N-1}$, with $q \geq q_0 > 0$, $s \geq s_0 > 0$. We define for $\theta > 1/2$ the Hilbert space

$$H^\theta_\theta(\Omega) = \{v \in H^\theta(\Omega), v_{|\Gamma} \in H^\theta(\Gamma)\},$$

with the scalar product

$$(w,v)_{H^\theta_\theta(\Omega)} = (w,v)_{H^\theta(\Omega)} + (qw,v)_{H^\theta(\Gamma)}.$$

We define the bilinear forms m on $H^1(\Omega)$ and a on $H^1_1(\Omega)$ by

$$m(w,v) = (w,v)_{L^2(\Omega)} + (qw,v)_{L^2(\Gamma)}$$

and

$$\begin{aligned} a(w,v) = &\int_\Omega \left(\frac{1}{2}((\boldsymbol{b}\cdot\nabla w)v - (\boldsymbol{b}\cdot\nabla v)w)\right) dx + \int_\Omega \nu\nabla w\cdot\nabla v\, dx \\ &+ \int_\Omega \left(c + \frac{1}{2}\nabla\cdot\boldsymbol{b}\right) wv\, dx + \int_\Gamma \left(\left(p - \frac{\boldsymbol{b}\cdot\boldsymbol{n}}{2} + \frac{q}{2}\nabla_\Gamma\cdot\boldsymbol{r}\right) wv \right. \\ &\left. + \frac{q}{2}(\nabla_\Gamma\cdot(\boldsymbol{r}w)v - \nabla_\Gamma\cdot(\boldsymbol{r}v)w) + qs\nabla_\Gamma w\cdot\nabla_\Gamma v\right) d\sigma. \end{aligned}$$

By the Green's formula, we can write a variational formulation of (2.1) in the form

$$\frac{d}{dt}\, m(w,v) + a(w,v) = (f,v)_{L^2(\Omega)} + (g,v)_{L^2(\Gamma)}. \tag{2.3}$$

THEOREM 2.1. *Suppose* $\nu \in W^{1,\infty}(\Omega)$*,* $\boldsymbol{b} \in (W^{1,\infty}(\Omega))^N$*,* $c \in L^\infty(\Omega)$*,* $p \in L^\infty(\Gamma)$*,* $q \in L^\infty(\Gamma)$*,* $\boldsymbol{r} \in (W^{1,\infty}(\Gamma))^{N-1}$*,* $s \in W^{1,\infty}(\Gamma)$*, with* $s \geq s_0 > 0$*,* $q \geq q_0 > 0$*, a.e. If* f *is in* $H^1(0,T;L^2(\Omega))$*,* u_0 *is in* $H^2_2(\Omega)$*, and* g *is in* $H^1((0,T);L^2(\Gamma))$*, the subdomain problem* (2.1) *has a unique solution* w *in* $L^\infty(0,T;H^2_2(\Omega))\cap W^{1,\infty}(0,T;L^2(\Omega))$ *with* $\partial_t w \in L^\infty(0,T;L^2(\Gamma))$*.*

Proof. The well-posedness relies on energy estimates and Grönwall's lemma, together with a Galerkin method as in [1,4,23]. In what follows, β, γ, δ, ζ denote positive real numbers depending only on the L^∞ norms of the coefficients $\boldsymbol{b}$, c, ν, p, q, $\boldsymbol{r}$ and the geometry. The basic estimate is obtained by multiplying the equation by w and integrating by parts in the domain, which gives

$$\frac{1}{2}\frac{d}{dt}m(w,w) \;+\; a(w,w) = (f,w)_{L^2(\Omega)} + (g,w)_{L^2(\Gamma)}.$$

With the assumptions on the coefficients, we can find $\alpha = \min(\nu_0, q_0 s_0)$ and $\beta > 0$ such that

$$\begin{aligned} a(w,w) = &\int_\Omega \nu|\nabla w|^2\, dx + \int_\Omega \left(c + \frac{1}{2}\nabla\cdot\boldsymbol{b}\right) w^2\, dx \\ &+ \int_\Gamma \left(\left(p - \frac{\boldsymbol{b}\cdot\boldsymbol{n}}{2} + \frac{q}{2}\nabla_\Gamma\cdot\boldsymbol{r}\right) w^2 + qs|\nabla_\Gamma w|^2\right) d\sigma \\ &\geq \alpha(\|\nabla w\|^2_{L^2(\Omega)} + \|\nabla_\Gamma w\|^2_{L^2(\Gamma)}) - \beta m(w,w). \end{aligned}$$

By the Cauchy–Schwarz inequality

$$(f,w)_{L^2(\Omega)} + (g,w)_{L^2(\Gamma)} \leq \frac{1}{2}m(w,w) + \frac{1}{2}\left(\|f\|^2_{L^2(\Omega)} + \frac{1}{q_0}\|g\|^2_{L^2(\Gamma)}\right).$$

Collecting these inequalities, we obtain

$$\frac{1}{2}\frac{d}{dt}m(w,w) \;+\; \alpha(\|\nabla w\|^2_{L^2(\Omega)} + \|\nabla_\Gamma w\|^2_{L^2(\Gamma)}) \\ \le \left(\beta + \frac{1}{2}\right) m(w,w) + \frac{1}{2}\left(\|f\|^2_{L^2(\Omega)} + \frac{1}{q_0}\|g\|^2_{L^2(\Gamma)}\right).$$

We now integrate in time and use Grönwall's lemma to obtain for any t in $(0,T)$

$$\begin{aligned} m(w(t),w(t)) \;+\; 2\alpha \int_0^t (\|\nabla w(s)\|^2_{L^2(\Omega)} + \|\nabla_\Gamma w(s)\|^2_{L^2(\Gamma)})ds \\ \le e^{(2\beta+1))t}\left(m(u_0,u_0) + \|f\|^2_{L^2(0,t;L^2(\Omega))} + \frac{1}{q_0}\|g\|^2_{L^2(0,t;L^2(\Gamma))}\right). \end{aligned} \tag{2.4}$$

We apply (2.4) to $\partial_t w$:

$$m(\partial_t w(t),\partial_t w(t)) \;+\; 2\alpha \int_0^t (\|\nabla \partial_t w(s)\|^2_{L^2(\Omega)} + \|\nabla_\Gamma \partial_t w(s)\|^2_{L^2(\Gamma)})ds \\ \le e^{(2\beta+1))t}\left(m(\partial_t w(0,\cdot),\partial_t w(0,\cdot)) + \|f_t\|^2_{L^2(0,t;L^2(\Omega))} + \frac{1}{q_0}\|g_t\|^2_{L^2(0,t;L^2(\Gamma))}\right).$$

We now use the equations at time 0 to estimate $m(\partial_t w(0,\cdot),\partial_t w(0,\cdot))$. From the equation in the domain, we deduce that there exists a constant γ such that

$$\|\partial_t w(0,\cdot)\|_{L^2(\Omega)} \le \gamma(\|u_0\|_{H^2(\Omega)} + \|f(0,\cdot)\|_{L^2(\Omega)}),$$

and from the boundary condition, using the evaluation of $\|\partial_n w\|_{L^2(\Gamma)}$ by $\|w\|_{H^2(\Omega)}$, that there exists a constant δ such that

$$\|\partial_t w(0,\cdot)\|_{L^2(\Gamma)} \le \delta(\|u_0\|_{H^2_2(\Omega)} + \|g(0,\cdot)\|_{L^2(\Gamma)}),$$

which gives altogether, with a new positive constant $\zeta > 0$,

$$\begin{aligned} m(\partial_t w(t),\partial_t w(t)) \;+\; 2\alpha \int_0^t (\|\nabla \partial_t w(s)\|^2_{L^2(\Omega)} + \|\nabla_\Gamma \partial_t w(s)\|^2_{L^2(\Gamma)})ds \\ \le \zeta e^{(2\beta+1)t}(\|u_0\|^2_{H^2_2(\Omega)} + \|f\|^2_{H^1(0,t;L^2(\Omega))} + \|g\|^2_{H^1(0,t;L^2(\Gamma))}). \end{aligned} \tag{2.5}$$

We can now apply the Galerkin method to find a unique solution w in $H^1(0,T;H^1_1(\Omega)) \cap W^{1,\infty}(0,T;L^2(\Omega)) \cap W^{1,\infty}(0,T;L^2(\Gamma))$. To obtain the H^2 regularity, we use that

$$\begin{aligned} -\Delta w &= \frac{1}{\nu}(f - \partial_t w - \nabla\cdot(\boldsymbol{b}w) + \nabla\nu\cdot\nabla w) \in L^\infty(0,T;L^2(\Omega)), \\ \nu\partial_{\boldsymbol{n}} w - qs\Delta_\Gamma w &= (\boldsymbol{b}\cdot\boldsymbol{n} - p)w - q\left(\partial_t w + \nabla_\Gamma\cdot(\boldsymbol{r}w) - \nabla_\Gamma s\cdot\nabla_\Gamma w\right) \\ &\quad + g \in L^\infty(0,T;L^2(\Gamma)), \end{aligned}$$

and we conclude as in [22, 23]. ∎

2.2. Convergence analysis.

THEOREM 2.2. *Assume $p_{i,j} \in W^{1,\infty}(\Omega_i)$, $p_{i,j} + p_{j,i} > 0$ a.e., $q_{i,j} = q > 0$, $\boldsymbol{b}_i \in (W^{1,\infty}(\Omega_i))^N$, $\nu_i \in W^{1,\infty}(\Omega_i)$, $\boldsymbol{r}_{i,j} \in (W^{1,\infty}(\Omega_i))^{N-1}$, with $\boldsymbol{r}_{i,j} = \boldsymbol{r}_{j,i}$ on $\Gamma_{i,j}$, and $s_{i,j} \in W^{1,\infty}(\Omega_i)$, $s_{i,j} > 0$ with $s_{i,j} = s_{j,i}$ on $\Gamma_{i,j}$. Then, algorithm* (1.3a) *converges in each subdomain to the solution u of problem* (1.1).

Proof. We first need some results in differential geometry. For any $i \in \{1, \dots, I\}$, for every $j \in \mathcal{N}_i$, the normal vector $\boldsymbol{n}_i$ can be extended in a neighborhood of $\Gamma_{i,j}$ in Ω_i as a smooth function $\tilde{\boldsymbol{n}}_i$ with length one. Let $\psi_{i,j} \in \mathcal{C}^\infty(\overline{\Omega_i})$, such that $\psi_{i,j} \equiv 1$ in a neighborhood of $\Gamma_{i,j}$, $\psi_{i,j} \equiv 0$ in a neighborhood of $\Gamma_{i,k}$ for $k \in \mathcal{N}_i$, $k \neq j$, and $\sum_{j\in\mathcal{N}_i} \psi_{i,j} > 0$ on Ω_i. We can assume that $\tilde{\boldsymbol{n}}_i$ is defined on a neighborhood of the support of $\psi_{i,j}$. We extend the tangential gradient and divergence operators in the support of $\psi_{i,j}$ by

$$\widetilde{\nabla}_{\Gamma_{i,j}}\varphi := \nabla\varphi - (\partial_{\tilde{\boldsymbol{n}}_i}\varphi)\tilde{\boldsymbol{n}}_i, \quad \widetilde{\nabla}_{\Gamma_{i,j}} \cdot \boldsymbol{\varphi} := \nabla \cdot (\boldsymbol{\varphi} - (\boldsymbol{\varphi}\cdot\tilde{\boldsymbol{n}}_i)\tilde{\boldsymbol{n}}_i).$$

It is easy to see that $(\widetilde{\nabla}_{\Gamma_{i,j}}\varphi)_{|\Gamma_{i,j}} = \nabla_{\Gamma_{i,j}}\varphi$, $(\widetilde{\nabla}_{\Gamma_{i,j}}\cdot\boldsymbol{\varphi})_{|\Gamma_{i,j}} = \nabla_{\Gamma_{i,j}}\cdot\boldsymbol{\varphi}$, and for $\boldsymbol{\varphi}$ and χ with support in $\mathrm{supp}(\psi_{i,j})$, we have

$$\int_{\Omega_i} (\widetilde{\nabla}_{\Gamma_{i,j}}\cdot\boldsymbol{\varphi})\,\chi\,dx = -\int_{\Omega_i} \boldsymbol{\varphi}\cdot\widetilde{\nabla}_{\Gamma_{i,j}}\chi\,dx. \tag{2.6}$$

Now we prove Theorem 2.2. We consider the algorithm (1.3a) on the error, so we suppose $f = u_0 = 0$. We set $\|\varphi\|_i = \|\varphi\|_{L^2(\Omega_i)}$, $\|\varphi\|_{i,\infty} = \|\varphi\|_{L^\infty(\Omega_i)}$, and $\|\varphi\|_{i,1,\infty} = \|\varphi\|_{W^{1,\infty}(\Omega_i)}$. We define $\beta_i = \sum_{j\in\mathcal{N}_i}\psi_{i,j}\beta_{i,j}$ with $\beta_{i,j} = \sqrt{\frac{1}{2}(p_{i,j}+p_{j,i})}$.

The key step is to write the energy estimate (2.23) on page 10, containing the boundary term

$$\int_0^t\int_{\Gamma_{i,j}} \left(\nu_i\partial_{\boldsymbol{n}_i}u_i^k - \boldsymbol{b}_i\cdot\boldsymbol{n}_iu_i^k + \mathcal{S}_{i,j}u_i^k\right)^2\,d\sigma\,d\tau,$$

and we will derive this by multiplying successively the first equation of (1.3a) by the terms $\beta_i^2\,u_i^k$, $\partial_t u_i^k$, $\widetilde{\nabla}_{\Gamma_{i,j}}\cdot(\psi_{i,j}^2\boldsymbol{r}_{i,j}u_i^k)$, and $-\widetilde{\nabla}_{\Gamma_{i,j}}\cdot(\psi_{i,j}^2 s_{i,j}\,\widetilde{\nabla}_{\Gamma_{i,j}}\,u_i^k)$.

• We multiply the first equation of (1.3a) by $\beta_i^2\,u_i^k$, integrate on $(0,t)\times\Omega_i$, and integrate by parts in space:

$$\begin{aligned}\frac{1}{2}\|\beta_iu_i^k(t)\|_i^2 &+ \int_0^t \|\sqrt{\nu_i}\,\nabla(\beta_iu_i^k)\|_i^2\,d\tau - \int_0^t\int_{\Omega_i}\beta_i(\boldsymbol{b}_i\cdot\nabla\beta_i)(u_i^k)^2\,dx\,d\tau\\ &+\int_0^t\int_{\Omega_i}\left(c_i+\frac{1}{2}\nabla\cdot\boldsymbol{b}_i\right)\beta_i^2(u_i^k)^2\,dx\,d\tau - \int_0^t\int_{\Omega_i}\nu_i|\nabla\beta_i|^2(u_i^k)^2\,dx\,d\tau\\ &- \sum_{j\in\mathcal{N}_i}\int_0^t\int_{\Gamma_{i,j}}\beta_{i,j}^2\left(\nu_i\partial_{\boldsymbol{n}_i}u_i^k - \frac{\boldsymbol{b}_i\cdot\boldsymbol{n}_i}{2}u_i^k\right)u_i^k\,d\sigma\,d\tau = 0.\end{aligned}\tag{2.7}$$

• We multiply the first equation of (1.3a) by $\partial_t u_i^k$, integrate on $(0,t)\times\Omega_i$, and then integrate by parts in space:

$$\begin{aligned}\int_0^t\|\partial_tu_i^k\|_i^2\,d\tau &+ \frac{1}{2}\|\sqrt{\nu_i}\,\nabla u_i^k(t)\|_i^2 + \int_0^t\int_{\Omega_i}(c_iu_i^k + \nabla\cdot(\boldsymbol{b}_iu_i^k))\,\partial_tu_i^k\,dx\,d\tau\\ &- \sum_{j\in\mathcal{N}_i}\int_0^t\int_{\Gamma_{i,j}}\nu_i\partial_{\boldsymbol{n}_i}u_i^k\,\partial_tu_i^k\,d\sigma\,d\tau = 0.\end{aligned}\tag{2.8}$$

• We multiply the first equation of (1.3a) by $\widetilde{\nabla}_{\Gamma_{i,j}}\cdot(\psi_{i,j}^2\boldsymbol{r}_{i,j}u_i^k)$, integrate on $(0,t)\times\Omega_i$, and integrate by parts in space:

$$\begin{aligned}(2.9)\qquad &\int_0^t \int_{\Omega_i} \left(\partial_t u_i^k + \nabla\cdot(\boldsymbol{b}_i u_i^k) + c_i u_i^k\right) \widetilde{\nabla}_{\Gamma_{i,j}} \cdot (\psi_{i,j}^2 \boldsymbol{r}_{i,j} u_i^k)\, dx\, d\tau \\ &+ \int_0^t \int_{\Omega_i} \nu_i \nabla u_i^k \cdot \nabla \left(\widetilde{\nabla}_{\Gamma_{i,j}} \cdot (\psi_{i,j}^2 \boldsymbol{r}_{i,j} u_i^k)\right) dx\, d\tau \\ &- \int_0^t \int_{\Gamma_{i,j}} \nu_i \partial_{\boldsymbol{n}_i} u_i^k\, \nabla_{\Gamma_{i,j}} \cdot (\boldsymbol{r}_{i,j} u_i^k)\, d\sigma\, d\tau = 0.\end{aligned}$$

We observe that

$$\begin{aligned}(2.10)\qquad &\int_0^t \int_{\Omega_i} \nu_i \nabla u_i^k \cdot \nabla \left(\widetilde{\nabla}_{\Gamma_{i,j}} \cdot (\psi_{i,j}^2 \boldsymbol{r}_{i,j} u_i^k)\right) dx\, d\tau \\ &= \int_0^t \int_{\Omega_i} \nu_i \nabla u_i^k \cdot \nabla \left(\widetilde{\nabla}_{\Gamma_{i,j}} \cdot (\psi_{i,j}^2 \boldsymbol{r}_{i,j}) u_i^k\right) dx\, d\tau \\ &\quad + \int_0^t \int_{\Omega_i} \nu_i \nabla u_i^k \cdot \nabla \left(\psi_{i,j}^2 \boldsymbol{r}_{i,j} \cdot \widetilde{\nabla}_{\Gamma_{i,j}}\, u_i^k\right) dx\, d\tau,\end{aligned}$$

with

$$\begin{aligned}(2.11)\quad &\int_0^t \int_{\Omega_i} \nu_i \nabla u_i^k \cdot \nabla \left(\psi_{i,j}^2 \boldsymbol{r}_{i,j} \cdot \widetilde{\nabla}_{\Gamma_{i,j}}\, u_i^k\right) dx\, d\tau \\ &\geq -\frac{1}{4} \int_0^t \|\psi_{i,j} \sqrt{\nu_i\, s_{i,j}}\; \nabla \widetilde{\nabla}_{\Gamma_{i,j}}\, u_i^k\|_i^2\, d\tau - C \int_0^t (\|\sqrt{\nu_i} \nabla u_i^k\|_i^2 + \|\beta_i u_i^k\|_i^2)\, d\tau.\end{aligned}$$

Replacing (2.11) in (2.10) and then (2.10) in (2.9), we obtain

$$\begin{aligned}(2.12)\quad &\\ &\int_0^t \int_{\Omega_i} \left(\partial_t u_i^k + \nabla\cdot(\boldsymbol{b}_i u_i^k) + c_i u_i^k\right) \widetilde{\nabla}_{\Gamma_{i,j}} \cdot (\psi_{i,j}^2 \boldsymbol{r}_{i,j} u_i^k)\, dx\, d\tau \\ &\qquad - \frac{1}{4} \int_0^t \|\psi_{i,j} \sqrt{\nu_i\, s_{i,j}}\; \nabla \widetilde{\nabla}_{\Gamma_{i,j}}\, u_i^k\|_i^2\, d\tau - \int_0^t \int_{\Gamma_{i,j}} \nu_i \partial_{\boldsymbol{n}_i} u_i^k\, \nabla_{\Gamma_{i,j}} \cdot (\boldsymbol{r}_{i,j} u_i^k)\, d\sigma\, d\tau \\ &\quad \leq C \int_0^t (\|\sqrt{\nu_i} \nabla u_i^k\|_i^2 + \|\beta_i u_i^k\|_i^2)\, d\tau.\end{aligned}$$

• Now we multiply the first equation of (1.3a) by $-\widetilde{\nabla}_{\Gamma_{i,j}} \cdot (\psi_{i,j}^2 s_{i,j}\, \widetilde{\nabla}_{\Gamma_{i,j}}\, u_i^k)$, integrate on $(0,t)\times\Omega_i$, and integrate by parts in space:

$$\begin{aligned}(2.13)\quad &\frac{1}{2} \|\psi_{i,j} \sqrt{s_{i,j}}\, \widetilde{\nabla}_{\Gamma_{i,j}}\, u_i^k(t)\|_i^2 - \int_0^t \int_{\Omega_i} \nabla\cdot(\boldsymbol{b}_i u_i^k)\, \widetilde{\nabla}_{\Gamma_{i,j}} \cdot (\psi_{i,j}^2 s_{i,j}\, \widetilde{\nabla}_{\Gamma_{i,j}}\, u_i^k)\, dx\, d\tau \\ &\quad - \int_0^t \int_{\Omega_i} c_i u_i^k \widetilde{\nabla}_{\Gamma_{i,j}} \cdot (\psi_{i,j}^2 s_{i,j}\, \widetilde{\nabla}_{\Gamma_{i,j}}\, u_i^k)\, dx\, d\tau \\ &\quad - \int_0^t \int_{\Omega_i} \nu_i \nabla u_i^k \cdot \nabla (\widetilde{\nabla}_{\Gamma_{i,j}} \cdot (\psi_{i,j}^2 s_{i,j}\, \widetilde{\nabla}_{\Gamma_{i,j}}\, u_i^k))\, dx\, d\tau \\ &\quad + \int_0^t \int_{\Gamma_{i,j}} \nu_i \partial_{\boldsymbol{n}_i} u_i^k\, \nabla_{\Gamma_{i,j}} \cdot (s_{i,j}\, \nabla_{\Gamma_{i,j}}\, u_i^k)\, d\sigma\, d\tau = 0.\end{aligned}$$

We have

$$-\int_0^t \int_{\Omega_i} \nu_i \nabla u_i^k \cdot \nabla(\widetilde{\nabla}_{\Gamma_{i,j}} \cdot (\psi_{i,j}^2 s_{i,j}\, \widetilde{\nabla}_{\Gamma_{i,j}}\, u_i^k))\, dx\, d\tau$$

$$\geq \frac{1}{2} \int_0^t \|\psi_{i,j}\sqrt{\nu_i\, s_{i,j}}\, \nabla\widetilde{\nabla}_{\Gamma_{i,j}}\, u_i^k\|_i^2\, d\tau - C\int_0^t \|\sqrt{\nu_i}\nabla u_i^k\|_i^2\, d\tau. \tag{2.14}$$

Replacing (2.14) in (2.13) leads to

$$\begin{aligned}
&\frac{1}{2}\|\psi_{i,j}\sqrt{s_{i,j}}\, \widetilde{\nabla}_{\Gamma_{i,j}}\, u_i^k(t)\|_i^2 + \frac{1}{2}\int_0^t \|\psi_{i,j}\sqrt{\nu_i\, s_{i,j}}\, \nabla\widetilde{\nabla}_{\Gamma_{i,j}}\, u_i^k\|_i^2\, d\tau\\
&\quad - \int_0^t \int_{\Omega_i} c_i u_i^k \widetilde{\nabla}_{\Gamma_{i,j}} \cdot (\psi_{i,j}^2 s_{i,j}\, \widetilde{\nabla}_{\Gamma_{i,j}}\, u_i^k)\, dx\, d\tau\\
&\quad + \int_0^t \int_{\Gamma_{i,j}} \nu_i \partial_{\boldsymbol{n}_i} u_i^k\, \nabla_{\Gamma_{i,j}} \cdot (s_{i,j}\, \nabla_{\Gamma_{i,j}}\, u_i^k)\, d\sigma\, d\tau\\
&\leq \int_0^t \int_{\Omega_i} \nabla\cdot(\boldsymbol{b}_i u_i^k)\, \widetilde{\nabla}_{\Gamma_{i,j}} \cdot (\psi_{i,j}^2 s_{i,j}\, \widetilde{\nabla}_{\Gamma_{i,j}}\, u_i^k)\, dx\, d\tau + C\int_0^t \|\sqrt{\nu_i}\nabla u_i^k\|_i^2\, d\tau.
\end{aligned} \tag{2.15}$$

We multiply (2.8) by q, we sum (2.12) and (2.15) over the interfaces $j \in \mathcal{N}_i$ and multiply by q, and then we add the three equations with (2.7). We use $ab \leq \frac{a^2}{2\varepsilon} + \frac{\varepsilon}{2} b^2$ in the integral terms on the right-hand side, and we get

$$\begin{aligned}
&\frac{1}{2}\left(\|\beta_i u_i^k(t)\|_i^2 + q\|\sqrt{\nu_i}\, \nabla u_i^k(t)\|_i^2 + q\sum_{j\in\mathcal{N}_i} \|\psi_{i,j}\sqrt{s_{i,j}}\, \widetilde{\nabla}_{\Gamma_{i,j}}\, u_i^k(t)\|_i^2 \right)\\
&\quad + \int_0^t \|\sqrt{\nu_i}\, \nabla(\beta_i u_i^k)\|_i^2\, d\tau + q\int_0^t \|\partial_t u_i^k\|_i^2\, d\tau\\
&\quad + \frac{q}{4}\sum_{j\in\mathcal{N}_i} \int_0^t \|\psi_{i,j}\sqrt{\nu_i\, s_{i,j}}\, \nabla\widetilde{\nabla}_{\Gamma_{i,j}}\, u_i^k\|_i^2\, d\tau\\
&\quad - \sum_{j\in\mathcal{N}_i} \int_0^t \int_{\Gamma_{i,j}} \beta_{i,j}^2 \left(\nu_i \partial_{\boldsymbol{n}_i} u_i^k - \frac{\boldsymbol{b}_i\cdot\boldsymbol{n}_i}{2} u_i^k \right) u_i^k\, d\sigma\, d\tau\\
&\quad - q\sum_{j\in\mathcal{N}_i} \int_0^t \int_{\Gamma_{i,j}} \nu_i \partial_{\boldsymbol{n}_i} u_i^k\, \left(\partial_t u_i^k + \nabla_{\Gamma_{i,j}} \cdot (\boldsymbol{r}_{i,j} u_i^k) - \nabla_{\Gamma_{i,j}} \cdot (s_{i,j}\, \nabla_{\Gamma_{i,j}}\, u_i^k) \right) d\sigma\, d\tau\\
&\leq q\sum_{j\in\mathcal{N}_i} \|\psi_{i,j}^2 \boldsymbol{r}_{i,j}\|_{i,1,\infty} \int_0^t \|u_i^k\|_i\, \|\partial_t u_i^k\|_i\, d\tau\\
&\quad + q\left(\|\boldsymbol{b}_i\|_{i,\infty} + \sum_{j\in\mathcal{N}_i} \|\psi_{i,j}^2 \boldsymbol{r}_{i,j}\|_{i,\infty} \right) \int_0^t \|\nabla u_i^k\|_i\, \|\partial_t u_i^k\|_i\, d\tau\\
&\quad + q\sum_{j\in\mathcal{N}_i} \|\boldsymbol{b}_i\|_{i,\infty} \sum_{j\in\mathcal{N}_i} \int_0^t \|\nabla u_i^k\|_i\, \|\widetilde{\nabla}_{\Gamma_{i,j}} \cdot (\psi_{i,j}^2 s_{i,j}\, \widetilde{\nabla}_{\Gamma_{i,j}}\, u_i^k)\|_i\, d\tau\\
&\quad + q(\|\boldsymbol{b}_i\|_{i,1,\infty} + \|c_i\|_{i,\infty}) \sum_{j\in\mathcal{N}_i} \int_0^t \|u_i^k\|_i\, \|\widetilde{\nabla}_{\Gamma_{i,j}} \cdot (\psi_{i,j}^2 s_{i,j}\, \widetilde{\nabla}_{\Gamma_{i,j}}\, u_i^k)\|_i\, d\tau\\
&\quad + \frac{q}{2}(\|\boldsymbol{b}_i\|_{i,1,\infty} + \|c_i\|_{i,\infty})\|u_i^k(t)\|_i^2 + C\left(\int_0^t \|\beta_i u_i^k\|_i^2\, d\tau + q\int_0^t \|\sqrt{\nu_i}\nabla u_i^k\|_i^2\, d\tau \right).
\end{aligned}$$

We bound the right-hand side by

$$\frac{1}{2}\left(\frac{q}{2}\int_0^t \|\partial_t u_i^k\|_i^2\,d\tau + \frac{q}{4}\sum_{j\in\mathcal{N}_i}\int_0^t \|\psi_{i,j}\sqrt{\nu_i\, s_{i,j}}\;\nabla\widetilde{\nabla}_{\Gamma_{i,j}}\,u_i^k\|_i^2\,d\tau\right)$$
$$+\frac{q}{2}(\|\boldsymbol{b}_i\|_{i,1,\infty}+\|c_i\|_{i,\infty})\|u_i^k(t)\|_i^2 + C\left(\int_0^t \|\beta_i u_i^k\|_i^2\,d\tau + q\int_0^t \|\sqrt{\nu_i}\nabla u_i^k\|_i^2\,d\tau\right).$$

We simplify the terms which appear on both sides and obtain

(2.16)
$$\begin{aligned}
&\frac{1}{2}\left(\|\beta_i u_i^k(t)\|_i^2 + q\|\sqrt{\nu_i}\,\nabla u_i^k(t)\|_i^2 + q\sum_{j\in\mathcal{N}_i}\|\psi_{i,j}\sqrt{s_{i,j}}\,\widetilde{\nabla}_{\Gamma_{i,j}}\,u_i^k(t)\|_i^2\right)\\
&\quad+\int_0^t \|\sqrt{\nu_i}\,\nabla(\beta_i u_i^k)\|_i^2\,d\tau + \frac{q}{2}\int_0^t \|\partial_t u_i^k\|_i^2\,d\tau\\
&\quad+\frac{q}{8}\sum_{j\in\mathcal{N}_i}\int_0^t \|\psi_{i,j}\sqrt{\nu_i\, s_{i,j}}\;\nabla\widetilde{\nabla}_{\Gamma_{i,j}}\,u_i^k\|_i^2\,d\tau\\
&\quad-\sum_{j\in\mathcal{N}_i}\int_0^t\int_{\Gamma_{i,j}}\beta_{i,j}^2\left(\nu_i\partial_{\boldsymbol{n}_i}u_i^k - \frac{\boldsymbol{b}_i\cdot\boldsymbol{n}_i}{2}u_i^k\right)u_i^k\,d\sigma\,d\tau\\
&\quad-q\sum_{j\in\mathcal{N}_i}\int_0^t\int_{\Gamma_{i,j}}\nu_i\partial_{\boldsymbol{n}_i}u_i^k\,\left(\partial_t u_i^k + \nabla_{\Gamma_{i,j}}\cdot(\boldsymbol{r}_{i,j}u_i^k) - \nabla_{\Gamma_{i,j}}\cdot(s_{i,j}\,\nabla_{\Gamma_{i,j}}\,u_i^k)\right)\,d\sigma\,d\tau\\
&\le\frac{q}{2}(\|\boldsymbol{b}_i\|_{i,1,\infty}+\|c_i\|_{i,\infty})\|u_i^k(t)\|_i^2 + C\left(\int_0^t \|\beta_i u_i^k\|_i^2\,d\tau + q\int_0^t \|\sqrt{\nu_i}\nabla u_i^k\|_i^2\,d\tau\right).
\end{aligned}$$

Recalling that $s_{i,j}=s_{j,i}$ on $\Gamma_{i,j}$ and $\boldsymbol{r}_{i,j}=\boldsymbol{r}_{j,i}$ on $\Gamma_{i,j}$, we now use

(2.17)
$$\begin{aligned}
&\frac{1}{4}\left(\nu_i\partial_{\boldsymbol{n}_i}u_i^k - \boldsymbol{b}_i\cdot\boldsymbol{n}_i u_i^k + \mathcal{S}_{i,j}u_i^k\right)^2 - \frac{1}{4}\left(\nu_i\partial_{\boldsymbol{n}_i}u_i^k - \boldsymbol{b}_i\cdot\boldsymbol{n}_i u_i^k - \mathcal{S}_{j,i}u_i^k\right)^2\\
&\quad=\beta_{i,j}^2\left(\nu_i\partial_{\boldsymbol{n}_i}u_i^k - \frac{\boldsymbol{b}_i\cdot\boldsymbol{n}_i}{2}u_i^k\right)u_i^k + q\nu_i\partial_{\boldsymbol{n}_i}u_i^k(\partial_t u_i^k\\
&\qquad+\nabla_{\Gamma_{i,j}}\cdot(\boldsymbol{r}_{i,j}u_i^k) - \nabla_{\Gamma_{i,j}}\cdot(s_{i,j}\,\nabla_{\Gamma_{i,j}}\,u_i^k))\\
&\qquad+\frac{q}{2}(p_{i,j}-p_{j,i}-2\boldsymbol{b}_i\cdot\boldsymbol{n}_i)(\partial_t u_i^k + \nabla_{\Gamma_{i,j}}\cdot(\boldsymbol{r}_{i,j}u_i^k) - \nabla_{\Gamma_{i,j}}\cdot(s_{i,j}\,\nabla_{\Gamma_{i,j}}\,u_i^k))u_i^k\\
&\qquad+\frac{1}{4}(p_{i,j}+p_{j,i})(p_{i,j}-p_{j,i}-\boldsymbol{b}_i\cdot\boldsymbol{n}_i)(u_i^k)^2.
\end{aligned}$$

Replacing (2.17) into (2.16), we obtain

$$\begin{aligned}
(2.18)\qquad&\frac{1}{2}\left(\|\beta_i u_i^k(t)\|_i^2 + q\|\sqrt{\nu_i}\,\nabla u_i^k(t)\|_i^2 + q\sum_{j\in\mathcal{N}_i}\|\psi_{i,j}\sqrt{s_{i,j}}\,\widetilde{\nabla}_{\Gamma_{i,j}}\,u_i^k(t)\|_i^2\right)\\
&\quad+\int_0^t \|\sqrt{\nu_i}\,\nabla(\beta_i u_i^k)\|_i^2\,d\tau + \frac{q}{2}\int_0^t \|\partial_t u_i^k\|_i^2\,d\tau\\
&\quad+\frac{1}{4}\sum_{j\in\mathcal{N}_i}\int_0^t\int_{\Gamma_{i,j}}\left(\nu_i\partial_{\boldsymbol{n}_i}u_i^k - \boldsymbol{b}_i\cdot\boldsymbol{n}_i\,u_i^k - \mathcal{S}_{j,i}u_i^k\right)^2\,d\sigma\,d\tau
\end{aligned}$$

$$+ \frac{q}{8} \sum_{j\in\mathcal{N}_i} \int_0^t \|\psi_{i,j}\sqrt{\nu_i\, s_{i,j}}\ \nabla\widetilde{\nabla}_{\Gamma_{i,j}}\, u_i^k\|_i^2\, d\tau$$

$$\le \frac{1}{4} \sum_{j\in\mathcal{N}_i} \int_0^t \int_{\Gamma_{i,j}} \left(\nu_i \partial_{\boldsymbol{n}_i} u_i^k - \boldsymbol{b}_i\cdot\boldsymbol{n}_i\, u_i^k + \mathcal{S}_{i,j} u_i^k\right)^2\, d\sigma\, d\tau$$

$$+ \frac{1}{4} \sum_{j\in\mathcal{N}_i} \int_0^t \int_{\Gamma_{i,j}} (p_{i,j}+p_{j,i})(-p_{i,j}+p_{j,i}+\boldsymbol{b}_i\cdot\boldsymbol{n}_i)(u_i^k)^2\, d\sigma\, d\tau$$

$$+ \frac{q}{2}(\|\boldsymbol{b}_i\|_{i,1,\infty} + \|c_i\|_{i,\infty})\|u_i^k(t)\|_i^2$$

$$+ \frac{q}{2} \sum_{j\in\mathcal{N}_i} \int_0^t \int_{\Gamma_{i,j}} (-p_{i,j}+p_{j,i}+2\boldsymbol{b}_i\cdot\boldsymbol{n}_i)(\partial_t u_i^k + \nabla_{\Gamma_{i,j}}\cdot(\boldsymbol{r}_{i,j}u_i^k)$$

$$- \nabla_{\Gamma_{i,j}}\cdot(s_{i,j}\,\nabla_{\Gamma_{i,j}}\, u_i^k))\, u_i^k\, d\sigma\, d\tau$$

$$+ C\left(\int_0^t \|\beta_i u_i^k\|_i^2\, d\tau + q\int_0^t \|\sqrt{\nu_i}\nabla u_i^k\|_i^2\, d\tau\right).$$

In order to estimate the fourth term on the right-hand side of (2.18), we observe that

$$\int_0^t \int_{\Gamma_{i,j}} (-p_{i,j}+p_{j,i}+2\boldsymbol{b}_i\cdot\boldsymbol{n}_i)u_i^k\,\partial_t u_i^k\, d\sigma\, d\tau = \frac{1}{2}\int_{\Gamma_{i,j}} (-p_{i,j}+p_{j,i}+2\boldsymbol{b}_i\cdot\boldsymbol{n}_i)u_i^k(t)^2\, d\sigma.$$

By the trace theorem on the right-hand side, we write

$$\int_0^t \int_{\Gamma_{i,j}} (-p_{i,j}+p_{j,i}+2\boldsymbol{b}_i\cdot\boldsymbol{n}_i)u_i^k\,\partial_t u_i^k\, d\sigma\, d\tau \le C\|u_i^k(t)\|_i\|\sqrt{\nu_i}\nabla u_i^k(t)\|_i$$

and obtain

$$\frac{q}{2}\int_0^t \int_{\Gamma_{i,j}} (-p_{i,j}+p_{j,i}+2\boldsymbol{b}_i\cdot\boldsymbol{n}_i)u_i^k\,\partial_t u_i^k\, d\sigma\, d\tau \le C\|u_i^k(t)\|_i^2 + \frac{q}{4}\|\sqrt{\nu_i}\nabla u_i^k(t)\|_i^2.$$

Noticing that

$$\|u_i^k(t)\|_i^2 = 2\int_0^t \int_{\Omega_i} (\partial_t u_i^k)u_i^k \le 2\left(\int_0^t \|\partial_t u_i^k\|_i^2\right)^{\frac{1}{2}}\left(\int_0^t \|u_i^k\|_i^2\right)^{\frac{1}{2}}, \tag{2.19}$$

we obtain

$$\frac{q}{2}\int_0^t \int_{\Gamma_{i,j}} (-p_{i,j}+p_{j,i}+2\boldsymbol{b}_i\cdot\boldsymbol{n}_i)u_i^k\,\partial_t u_i^k\, d\sigma\, d\tau \tag{2.20}$$
$$\le \frac{q}{8}\int_0^t \|\partial_t u_i^k\|_i^2\, d\tau + \frac{q}{4}\|\sqrt{\nu_i}\,\nabla u_i^k(t)\|_i^2 + C\left(\int_0^t \|\beta_i u_i^k\|_i^2\, d\tau\right).$$

Moreover, integrating by parts and using the trace theorem, we have

(2.21)
$$-\frac{q}{2}\int_0^t \int_{\Gamma_{i,j}} \nabla_{\Gamma_{i,j}}\cdot(s_{i,j}\,\nabla_{\Gamma_{i,j}}\, u_i^k)(-p_{i,j}+p_{j,i}+2\boldsymbol{b}_i\cdot\boldsymbol{n}_i)u_i^k\, d\sigma\, d\tau$$
$$\le \frac{q}{16}\int_0^t \|\psi_{i,j}\sqrt{\nu_i\, s_{i,j}}\ \nabla\widetilde{\nabla}_{\Gamma_{i,j}}\, u_i^k\|_i^2\, d\tau + C\left(\int_0^t \|\widetilde{\nabla}_{\Gamma_{i,j}}\, u_i^k\|_i^2\, d\tau + \int_0^t \|\beta_i u_i^k\|_i^2\, d\tau\right).$$

Using (2.19), we estimate the third term on the right-hand side of (2.18) by

$$\frac{q}{2}(\|\boldsymbol{b}_i\|_{i,1,\infty} + \|c_i\|_{i,\infty})\|u_i^k(t)\|_i^2 \leq \frac{q}{8}\int_0^t \|\partial_t u_i^k\|_i^2\, d\tau + C\int_0^t \|\beta_i u_i^k\|_i^2\, d\tau. \tag{2.22}$$

Replacing (2.20), (2.21), and (2.22) in (2.18), we obtain the following energy estimate:

$$\begin{aligned}
&\frac{1}{2}\left(\|\beta_i u_i^k(t)\|_i^2 + \frac{q}{2}\|\sqrt{\nu_i}\,\nabla u_i^k(t)\|_i^2 + q\sum_{j\in\mathcal{N}_i}\|\psi_{i,j}\sqrt{s_{i,j}}\,\widetilde{\nabla}_{\Gamma_{i,j}}\, u_i^k(t)\|_i^2\right)\\
&\quad + \int_0^t \|\sqrt{\nu_i}\,\nabla(\beta_i u_i^k)\|_i^2\, d\tau + \frac{q}{4}\int_0^t \|\partial_t u_i^k\|_i^2\, d\tau\\
&\quad + \frac{q}{16}\sum_{j\in\mathcal{N}_i}\int_0^t \|\psi_{i,j}\sqrt{\nu_i\, s_{i,j}}\ \nabla\,\widetilde{\nabla}_{\Gamma_{i,j}}\, u_i^k\|_i^2\, d\tau\\
&\quad + \frac{1}{4}\sum_{j\in\mathcal{N}_i}\int_0^t\int_{\Gamma_{i,j}}\left(\nu_i\partial_{\boldsymbol{n}_i} u_i^k - \boldsymbol{b}_i\cdot\boldsymbol{n}_i\, u_i^k - \mathcal{S}_{j,i}u_i^k\right)^2\, d\sigma\, d\tau\\
&\leq \frac{1}{4}\sum_{j\in\mathcal{N}_i}\int_0^t\int_{\Gamma_{i,j}}\left(\nu_i\partial_{\boldsymbol{n}_i} u_i^k - \boldsymbol{b}_i\cdot\boldsymbol{n}_i\, u_i^k + \mathcal{S}_{i,j}u_i^k\right)^2\, d\sigma\, d\tau\\
&\quad + C\left(\int_0^t \|\beta_i u_i^k\|_i^2\, d\tau + \frac{q}{2}\int_0^t \|\sqrt{\nu_i}\,\nabla u_i^k\|_i^2\, d\tau\right).
\end{aligned}$$

Then, using the transmission conditions, we have

$$\begin{aligned}
&\frac{1}{2}\left(\|\beta_i u_i^k(t)\|_i^2 + \frac{q}{2}\|\sqrt{\nu_i}\,\nabla u_i^k(t)\|_i^2 + q\sum_{j\in\mathcal{N}_i}\|\psi_{i,j}\sqrt{s_{i,j}}\,\widetilde{\nabla}_{\Gamma_{i,j}}\, u_i^k(t)\|_i^2\right)\\
&\quad + \int_0^t \|\sqrt{\nu_i}\,\nabla(\beta_i u_i^k)\|_i^2\, d\tau + \frac{q}{4}\int_0^t \|\partial_t u_i^k\|_i^2\, d\tau\\
&\quad + \frac{q}{16}\sum_{j\in\mathcal{N}_i}\int_0^t \|\psi_{i,j}\sqrt{\nu_i\, s_{i,j}}\ \nabla\,\widetilde{\nabla}_{\Gamma_{i,j}}\, u_i^k\|_i^2\, d\tau\\
&\quad + \frac{1}{4}\sum_{j\in\mathcal{N}_i}\int_0^t\int_{\Gamma_{i,j}}\left(\nu_i\partial_{\boldsymbol{n}_i} u_i^k - \boldsymbol{b}_i\cdot\boldsymbol{n}_i\, u_i^k - \mathcal{S}_{j,i}u_i^k\right)^2\, d\sigma\, d\tau\\
&\leq \frac{1}{4}\sum_{j\in\mathcal{N}_i}\int_0^t\int_{\Gamma_{i,j}}\left(\nu_j\partial_{\boldsymbol{n}_i} u_j^{k-1} - \boldsymbol{b}_j\cdot\boldsymbol{n}_i\, u_j^{k-1} + \mathcal{S}_{i,j}u_j^{k-1}\right)^2\, d\sigma\, d\tau\\
&\quad + C\left(\int_0^t \|\beta_i u_i^k\|_i^2\, d\tau + \frac{q}{2}\int_0^t \|\sqrt{\nu_i}\,\nabla u_i^k\|_i^2\, d\tau\right).
\end{aligned} \tag{2.23}$$

We now sum over the subdomains for $1 \leq i \leq I$, and on the iterations for $1 \leq k \leq K$ the boundary terms cancel out, and we obtain for any $t \in (0, T)$

$$\begin{aligned}
&\sum_{k=1}^K\sum_{i=1}^I\left(\|\beta_i u_i^k(t)\|_i^2 + q\|\sqrt{\nu_i}\,\nabla u_i^k(t)\|_i^2 + \nu_0\int_0^t \|\nabla(\beta_i u_i^k)\|_i^2\, d\tau\right)\\
&\qquad \leq \alpha(t) + C\sum_{k=1}^K\sum_{i=1}^I\left(\int_0^t \|\beta_i u_i^k\|_i^2\, d\tau + q\int_0^t \|\sqrt{\nu_i}\,\nabla u_i^k\|_i^2\, d\tau\right),
\end{aligned} \tag{2.24}$$

with

$$\alpha(t) = \frac{1}{4}\sum_{i=1}^{I}\sum_{j\in\mathcal{N}_i}\int_0^t\int_{\Gamma_{i,j}}\left(\nu_j\partial_{\boldsymbol{n}_i}u_j^0 - \boldsymbol{b}_j\cdot\boldsymbol{n}_i\,u_j^0 + \mathcal{S}_{i,j}u_j^0\right)^2\,d\sigma\,d\tau. \tag{2.25}$$

We now apply Grönwall's lemma and obtain that for any $K > 0$

$$\sum_{k=1}^{K}\sum_{i=1}^{I}\|u_i^k(t)\|_{H^1(\Omega_i)}^2 \le \alpha(T)e^{C_1T},$$

which proves that the sequence u_i^k converges to zero in $L^\infty(0,T;H^1(\Omega_i))$ for each i and concludes the proof of the theorem. ◻

3. The discontinuous Galerkin time stepping for the Schwarz waveform relaxation algorithm.

3.1. Local problem (2.1): Time discontinuous Galerkin method. We recall the time discontinuous Galerkin method as presented in [15]. We are given a decomposition $\mathcal{T}$ of the time interval $(0,T)$, $I_n = (t_n, t_{n+1}]$ for $0 \le n \le N$; the mesh size is $k_n = t_{n+1} - t_n$. For $\mathcal{B}$ a Banach space and I an interval of $\mathbb{R}$, we define for any integer $d \ge 0$

$$\begin{aligned}
\mathbf{P}_d(\mathcal{B}) &= \left\{\varphi : I \to \mathcal{B},\ \varphi(t) = \sum_{i=0}^{d}\varphi_i t^i,\ \varphi_i \in \mathcal{B}\right\},\\
\mathcal{P}_d(\mathcal{B},\mathcal{T}) &= \{\varphi : I \to \mathcal{B},\ \varphi_{|I_n} \in \mathbf{P}_d(\mathcal{B}),\ 1 \le n \le N\}.
\end{aligned}$$

Let $\mathcal{B} = H_1^1(\Omega)$. We define an approximation U of u, a polynomial of degree lower than d on every subinterval I_n. For every point t_n, we define $U(t_n^-) = \lim_{t\to t_n-0} U(t)$ and $U(t_n^+) = \lim_{t\to t_n+0} U(t)$. We use the weak formulation (2.3), and we search for $U \in \mathcal{P}_d(\mathcal{B},\mathcal{T})$ such that

$$\begin{cases}
U(0,\cdot) = u_0,\\
\forall\, V \in \mathcal{P}_d(\mathcal{B},\mathcal{T})\colon\ \displaystyle\int_{I_n}(\,m(\dot{U},V) + a(U,V))\,dt\\
\qquad\qquad + m(U(t_n^+,\cdot) - U(t_n^-,\cdot), V(t_n^+,\cdot)) = \displaystyle\int_{I_n} L(V)\,dt,
\end{cases} \tag{3.1}$$

with $L(V) = (f,V)_{L^2(\Omega)} + (g,V)_{L^2(\Gamma)}$. Since I_n is closed at t_{n+1}, $U(t_{n+1}^-)$ is the value of U at t_{n+1}. Due to the discontinuous nature of the test and trial spaces, the method is an implicit time stepping scheme, and $U \in \mathbf{P}_d(\mathcal{B},\mathcal{T})$ is obtained recursively on each subinterval, which makes it very flexible.

The well-posedness of (3.1) is addressed in section 3.2 through the proof of the convergence of the algorithm in the semidiscrete case.

We will make use of the following remark [17]. We introduce the Gauss–Radau points $(0 < \tau_1, \ldots, \tau_{d+1} = 1)$, defined such that the quadrature formula

$$\int_0^1 f(t)dt \approx \sum_{j=1}^{d+1} w_q\ f(\tau_q)$$

is exact in $\mathbf{P}_{2d}$, and the interpolation operator $\mathcal{I}_n$ on $[t_n, t_{n+1}]$ at points $(t_n, t_n + \tau_1 k_n, \ldots, t_n + \tau_{d+1}k_n)$. For any $\chi \in \mathbf{P}_d$, $\hat{\chi} = \mathcal{I}_n\chi \in \mathbf{P}_{d+1}$.

Let $\mathcal{I} : \mathcal{P}_d(\mathcal{B},\mathcal{T}) \to \mathcal{P}_{d+1}(\mathcal{B},\mathcal{T})$ be the operator whose restriction to each subinterval is $\mathcal{I}_n$ and satisfies $\mathcal{I}U(t_n^+) = U(t_n^-)$. By using the Gauss–Radau formula, which is exact in $\mathbf{P}_{2d}$, we have for all $\psi_{i,j} \in \mathbf{P}_d$

$$\int_{I_n} \frac{d\mathcal{I}\chi}{dt}\,\psi_{i,j}\,dt - \int_{I_n} \frac{d\chi}{dt}\,\psi_{i,j}\,dt = (\chi(t_n^+) - \chi(t_n^-))\psi_{i,j}(t_n^+).$$

As a consequence, we have a very useful inequality:

$$\int_{I_n} \frac{d}{dt}(\mathcal{I}\psi_{i,j})\psi_{i,j}dt \geq \frac{1}{2}[\psi_{i,j}(t_{n+1}^-)^2 - \psi_{i,j}(t_n^-)^2]. \tag{3.2}$$

Also, (3.1) can be rewritten as

$$\int_{I_n} \left(m\left(\frac{d\mathcal{I}U}{dt}, V\right) + a(U,V)\right) dt = \int_{I_n} L(V)\,dt, \tag{3.3}$$

or, in the strong formulation,

$$\begin{aligned} &\partial_t(\mathcal{I}U) + \nabla\cdot(\boldsymbol{b}U - \nu\nabla U) + cU = \Pi f \text{ in } \Omega\times(0,T),\\ &\big(\nu\,\partial_{\boldsymbol{n}} - \boldsymbol{b}\cdot\boldsymbol{n}\big)U + p\,U + q(\partial_t(\mathcal{I}U) + \nabla_\Gamma\cdot(\boldsymbol{r}U - s\nabla_\Gamma U)) = \Pi g \text{ on } \Gamma\times(0,T), \end{aligned} \tag{3.4}$$

where Π is the projection L^2 in each subinterval of $\mathcal{T}$ on $\mathbf{P}_d$. This problem belongs to the large class of problems considered in [24], for which optimal error estimates are given as follows.

THEOREM 3.1. *Let U be the solution of* (3.1) *and u the solution of* (2.1)*. Under the assumptions of Theorem* 2.1*, the estimate*

$$\|u - U\|_{L^\infty(I_n, L^2(\Omega))} \leq C\Delta t^{\,d+1}\|\partial_t^{d+1}u\|_{L^2(0,T;H_2^2(\Omega))} \tag{3.5}$$

holds with $\Delta t = \max_{0\leq n\leq N} k_n$.

3.2. The discrete in time optimized Schwarz waveform relaxation algorithm with different subdomains grids. The time partition in subdomain Ω_i is $\mathcal{T}_i$, with N_i+1 intervals I_n^i, and time steps k_n^i. In view of formulation (3.4), we define interpolation operators $\mathcal{I}^i$ and projection operators Π^i in each subdomain, i.e., Π^i is the L^2 projection in each subinterval of $\mathcal{T}_i$ on $\mathbf{P}_d$, and we solve

$$\partial_t(\mathcal{I}^i U_i^k) + \nabla\cdot(\boldsymbol{b}_i U_i^k - \nu_i\nabla U_i^k) + c_i\,U_i^k = \Pi^i f \text{ in } \Omega_i\times(0,T), \tag{3.6a}$$

$$\big(\nu_i\partial_{\boldsymbol{n}_i} - \boldsymbol{b}_i\cdot\boldsymbol{n}_i\big)\,U_i^k + S_{i,j}U_i^k = \Pi^i\big((\nu_j\partial_{\boldsymbol{n}_i} - \boldsymbol{b}_j\cdot\boldsymbol{n}_i)\,U_j^{k-1} + \widetilde{S}_{i,j}U_j^{k-1}\big) \quad \text{on } \Gamma_{i,j}, j\in\mathcal{N}_i, \tag{3.6b}$$

with

$$\begin{aligned} S_{i,j}U &= p_{i,j}\,U + q_{i,j}\,(\partial_t(\mathcal{I}^iU) + \nabla_{\Gamma_{i,j}}\cdot(\boldsymbol{r}_{i,j}U - s_{i,j}\nabla_{\Gamma_{i,j}}U)),\\ \widetilde{S}_{i,j}U &= p_{i,j}\,U + q_{i,j}\,(\partial_t(\mathcal{I}^jU) + \nabla_{\Gamma_{i,j}}\cdot(\boldsymbol{r}_{i,j}U - s_{i,j}\nabla_{\Gamma_{i,j}}U)). \end{aligned} \tag{3.7}$$

If the sequence U_i^k converges, the limit is a solution of

$$\partial_t(\mathcal{I}^i U_i) + \nabla\cdot(\boldsymbol{b}_i U_i - \nu_i\nabla U_i) + c_i\,U_i = \Pi^i f \text{ in } \Omega_i\times(0,T), \tag{3.8a}$$

$$\big(\nu_i\partial_{\boldsymbol{n}_i} - \boldsymbol{b}_i\cdot\boldsymbol{n}_i\big)\,U_i + S_{i,j}U_i = \Pi^i\big((\nu_j\partial_{\boldsymbol{n}_i} - \boldsymbol{b}_j\cdot\boldsymbol{n}_i)\,U_j + \widetilde{S}_{i,j}U_j\big) \quad \text{on } \Gamma_{i,j}, j\in\mathcal{N}_i. \tag{3.8b}$$

In the semidiscrete case, we cannot use the (discrete) Grönwall lemma as in the continuous case, due to the presence of the global in time projection operator $\mathcal{P}^j$ in the transmission conditions. Then, for general decompositions, the added geometrical terms in the estimates cannot be treated. Therefore, we restrict ourselves in what follows to a decomposition of the domain into strips with interfaces $\Gamma_{i,j}$ which are hyperplanes.

THEOREM 3.2. *Assume that $p_{i,j} = p > 0$, $q_{i,j} = q > 0$, $s_{i,j} = s > 0$, $c_i \geq 0$, $\boldsymbol{b}_i = 0$, and $\boldsymbol{r}_{i,j} = 0$. Problem* (3.8) *has a unique solution $(U_i)_{i\in I}$ and in each subdomain U_i is the limit of the iterates of algorithm* (3.6).

Proof. We consider the algorithm (3.6) on the error, so we suppose $f = u_0 = 0$. As in the continuous case, the proof is based on energy estimates containing the term

$$\int_{I_n^i}\int_{\Gamma_{i,j}} \left(\nu_i\partial_{\boldsymbol{n}_i}U_i^k + \mathcal{S}_{i,j}U_i^k\right)^2 \, d\sigma \, d\tau$$

and we derive this by multiplying successively the first equation of (3.6) by the terms U_i^k, $\partial_t(\mathcal{I}^i U_i^k)$, and $-\Delta_{\Gamma_{i,j}} U_i^k$. We set $||| \, \varphi \, |||_i^2 = \|\sqrt{\nu_i}\,\nabla\varphi\|^2_{L^2(\Omega_i)} + \|\sqrt{c_i}\,\varphi\|^2_{L^2(\Omega_i)}$. We multiply the first equation of (3.6) by U_i^k, integrate on $I_n^i \times \Omega_i$, and then integrate by parts in space and use (3.2):

$$\frac{1}{2}\|U_i^k(t_{n+1}^-)\|_i^2 + \int_{I_n^i} |||\, U_i^k \,|||_i^2 \, d\tau - \sum_{j\in\mathcal{N}_i}\int_{I_n^i}\int_{\Gamma_{i,j}} \nu_i\partial_{\boldsymbol{n}_i}U_i^k\,U_i^k\,d\sigma\,d\tau \leq \frac{1}{2}\|U_i^k(t_n^-)\|_i^2. \tag{3.9}$$

We multiply the first equation of (3.6) by $\partial_t(\mathcal{I}^i U_i^k)$, integrate on $I_n^i \times \Omega_i$, and then integrate by parts in space and use (3.2):

$$\begin{aligned}\frac{1}{2}\, |||\, U_i^k(t_{n+1}^-)\,|||_i^2 &+ \int_{I_n^i} \|\partial_t(\mathcal{I}^i U_i^k)\|_i^2 \, d\tau \\ &- \sum_{j\in\mathcal{N}_i}\int_{I_n^i}\int_{\Gamma_{i,j}} \nu_i\partial_{\boldsymbol{n}_i}U_i^k\,\partial_t(\mathcal{I}^i U_i^k)\,d\sigma\,d\tau \leq \frac{1}{2}\, |||\, U_i^k(t_n^-)\,|||_i^2 \,.\end{aligned} \tag{3.10}$$

Now we multiply the first equation of (3.6) by $-\Delta_{\Gamma_{i,j}} U_i^k$ integrate on $I_n^i \times \Omega_i$, and integrate by parts in space and use (3.2):

$$\begin{aligned}\frac{1}{2}\|\nabla_{\Gamma_{i,j}}U_i^k(t_{n+1}^-)\|_i^2 &+ \int_{I_n^i} |||\, \nabla_{\Gamma_{i,j}}U_i^k \,|||_i^2 \, d\tau \\ &+ \int_{I_n^i}\int_{\Gamma_{i,j}} \nu_i\partial_{\boldsymbol{n}_i}u_i^k\,\Delta_{\Gamma_{i,j}}\,u_i^k\,d\sigma\,d\tau \leq \frac{1}{2}\|\nabla_{\Gamma_{i,j}}U_i^k(t_n^-)\|_i^2,\end{aligned} \tag{3.11}$$

where we have used the fact that $\Delta_{\Gamma_{i,j}}$ is a constant coefficient operator. Let

$$E^n(U_i^k) = \frac{p}{2}\|U_i^k((t_n^i)^-)\|_i^2 + \frac{q}{2}\, |||\, U_i^k((t_n^i)^-)\,|||_i^2 + \frac{sq}{2}\sum_{j\in\mathcal{N}_i}\|\nabla_{\Gamma_{i,j}}U_i^k((t_n^i)^-)\|_i^2.$$

Multiplying (3.9) by p, (3.10) by q, and (3.11) by sq and adding the three equations, we get

$$E^{n+1}(U_i^k) + \int_{I_n^i} \left[p \,|||\, U_i^k \,|||_i^2 \, + q\|\partial_t(\mathcal{I}_n^i U_i^k)\|_i^2 \, + sq \sum_{j\in\mathcal{N}_i} |||\, \nabla_{\Gamma_{i,j}} U_i^k \,|||_i^2 \right] d\tau$$
$$- \sum_{j\in\mathcal{N}_i} \int_{I_n^i} \int_{\Gamma_{i,j}} \nu_i \partial_{\boldsymbol{n}_i} U_i^k \, S_{i,j} U_i^k \, d\sigma \, d\tau \le E^n(U_i^k).$$

It can be rewritten as

$$E^{n+1}(U_i^k) + \int_{I_n^i} \left[p \,|||\, U_i^k \,|||_i^2 \, + q\|\partial_t(\mathcal{I}_n^i U_i^k)\|_i^2 \, + sq \sum_{j\in\mathcal{N}_i} |||\, \nabla_{\Gamma_{i,j}} U_i^k \,|||_i^2 \right] d\tau$$
$$+ \frac{1}{4} \sum_{j\in\mathcal{N}_i} \int_{I_n^i} \int_{\Gamma_{i,j}} (\nu_i \partial_{\boldsymbol{n}_i} U_i^k - \, S_{i,j} U_i^k)^2 \, d\sigma \, d\tau$$
$$\le E^n(U_i^k) + \frac{1}{4} \sum_{j\in\mathcal{N}_i} \int_{I_n^i} \int_{\Gamma_{i,j}} (\nu_i \partial_{\boldsymbol{n}_i} U_i^k + \, S_{i,j} U_i^k)^2 \, d\sigma \, d\tau.$$

For $m \in \{0, \ldots, N\}$, we now sum in time for $0 \le n \le m$ and use the transmission condition. Since $E^0(U_i^k) = 0$, we obtain

(3.12)
$$E^{m+1}(U_i^k) + \int_0^{t_{m+1}} \left[p \,|||\, U_i^k \,|||_i^2 \, + q\|\partial_t(\mathcal{I}^i U_i^k)\|_i^2 \, + sq \sum_{j\in\mathcal{N}_i} |||\, \nabla_{\Gamma_{i,j}} U_i^k \,|||_i^2 \right] d\tau$$
$$+ \frac{1}{4} \sum_{j\in\mathcal{N}_i} \int_0^{t_{m+1}} \int_{\Gamma_{i,j}} (\nu_i \partial_{\boldsymbol{n}_i} U_i^k - \, S_{i,j} U_i^k)^2 \, d\sigma \, d\tau$$
$$\le \frac{1}{4} \sum_{j\in\mathcal{N}_i} \int_0^{t_{m+1}} \int_{\Gamma_{i,j}} (\Pi^i(-\nu_j \partial_{\boldsymbol{n}_j} U_j^{k-1} + \, \widetilde{S}_{i,j} U_j^{k-1}))^2 \, d\sigma \, d\tau.$$

We sum on the subdomains and use the fact that the projection is a contraction. Since we are in the case where $p_{i,j} = p$, $q_{i,j} = q$, $r_{i,j} = 0$, and $s_{i,j} = s$, we have $\widetilde{S}_{i,j} = S_{j,i}$. Thus, we can sum on the iterates, the boundary terms cancel out, and for all $m \in \{0, \ldots, N\}$ we obtain

(3.13)
$$\sum_{k=1}^{K} \sum_{i=1}^{I} \left(E^{m+1}(U_i^k) + \int_0^{t_{m+1}} \left[p \,|||\, U_i^k \,|||_i^2 \, + q\|\partial_t(\mathcal{I}^i U_i^k)\|_i^2 \, + sq \sum_{j\in\mathcal{N}_i} |||\, \nabla_{\Gamma_{i,j}} U_i^k \,|||_i^2 \right] d\tau \right)$$
$$+ \frac{1}{4} \sum_{i=1}^{I} \sum_{j\in\mathcal{N}_i} \int_0^{t_{m+1}} \int_{\Gamma_{i,j}} (\nu_i \partial_{\boldsymbol{n}_i} U_i^k - \, \mathcal{S}_{i,j} U_i^K)^2 \, d\sigma \, d\tau$$
$$\le \frac{1}{4} \sum_{i=1}^{I} \sum_{j\in\mathcal{N}_i} \int_0^{t_{m+1}} \int_{\Gamma_{i,j}} (\nu_i \partial_{\boldsymbol{n}_i} U_i^0 - \, \mathcal{S}_{i,j} U_i^0)^2 \, d\sigma \, d\tau.$$

We first apply this inequality to prove the first part of the theorem. Problem (3.8a)–(3.8b) is a square discrete system, and proving well-posedness is equivalent to proving uniqueness. Dropping the superscript in (3.12) gives $U_i((t_m^i)^-) = 0$ a.e. for each $m \in \{0,\dots,N\}$, and $\mathcal{I}^i U_i$ constant on each subinterval I_m for each $m \in \{0,\dots,N\}$. Therefore, U_i is constant on I_m, with $U_i((t_m^i)^-) = 0$, for all $m \in \{0,\dots,N\}$, and it gives the result. The convergence then results in similar arguments, and we obtain, for all $m \in \{0,\dots,N\}$, that $\sum_{i=1}^I \|U_i^k(t_{m+1})\|_i^2$ and $\sum_{i=1}^I \int_0^{t_{m+1}} ||| U_i^k |||_i^2 \, d\tau$ tends to zero as k tends to infinity. ∎

4. Numerical results. We have implemented the algorithm with $d = 1$ and $\mathbf{P}_1$ finite elements in space in each subdomain, extending the nonconforming approach in [6]. Time windows are used in order to reduce the number of iterations of the algorithm.

We consider two subdomains and perform all the iterations in an alternating fashion: at each iteration of algorithm (3.6a)–(3.6b), we first solve the subproblem in $\Omega_1 \times (0,T)$. Then we solve the subproblem in $\Omega_2 \times (0,T)$, replacing the transmission condition (3.6b) by

$$\left(\nu_2 \partial_{\boldsymbol{n}_2} - \boldsymbol{b}_2 \cdot \boldsymbol{n}_2\right) U_2^k + S_{2,1} U_2^k = \Pi^2\left(\left(\nu_1 \partial_{\boldsymbol{n}_2} - \boldsymbol{b}_1 \cdot \boldsymbol{n}_2\right) U_1^k + \widetilde{S}_{2,1} U_1^k\right) \text{ on } \Gamma_{1,2}.$$

For the free parameters defining $S_{i,j}$ and $\tilde{S}_{i,j}$, we chose $r_{i,j}$ to be the tangential component of the advection and $s_{i,j}$ the value of the diffusion in the domain Ω_j. The optimized parameters $p_{i,j}$ and $q_{i,j}$ are taken constant along the interface. We first compute for each edge on the grid on the interface $\Gamma_{i,j}$ parameters $p_{i,j}^*$ and $q_{i,j}^*$ obtained by a numerical optimization of the theoretical convergence factor [5, 10], adapted to anisotropic diffusion in section 4.3. Then $p_{i,j}$ and $q_{i,j}$ are defined as the mean value of all the $p_{i,j}^*$ and $q_{i,j}^*$, respectively.

4.1. An example of a multidomain solution with discontinuous coefficients. We first analyze the precision in time on an example with discontinuous variable diffusion. The advection velocity is also discontinuous, normal to the interface in one subdomain, and tangential to the interface in the other subdomain. This case of a flow tangential to the interface may lead to very slow convergence of the Schwarz algorithm when the interface conditions are not related to the convergence factor of the domain decomposition method (see, for example, [13]).

The physical domain is $\Omega = (0,1) \times (0,2)$, and the final time is $T = 1$. The initial value is $u_0 = 0.25 e^{-100((x-0.55)^2+(y-1.7)^2)}$, and the right-hand side is $f = 0$. The domain Ω is split into two subdomains $\Omega_1 = (0, 0.5) \times (0,2)$ and $\Omega_2 = (0.5, 1) \times (0,2)$. The reaction c is zero, the advection and diffusion coefficients are $\boldsymbol{b}_1 = (0,-1)$, $\nu_1 = 0.001\sqrt{y}$ and $\boldsymbol{b}_2 = (-0.1, 0)$, $\nu_2 = 0.1 \sin(xy)$.

The space mesh is conforming, and the process is stopped when the residual is smaller than 10^{-8}. We compute a variational reference solution on a time grid with 4096 time steps. The nonconforming solutions are interpolated on the previous grid to compute the error. We start with a time grid with 128 time steps for the left domain and 94 time steps for the right domain. Thereafter the time step is divided by 2 several times. Figure 4.1 shows the norms of the error in $L^\infty(I, L^2(\Omega_i))$ versus the number of refinements for both subdomains. First we observe the order 2 in time for the nonconforming case. This fits the theoretical estimates (3.5). Moreover, the error obtained in the nonconforming case, in the subdomain where the grid is finer, is nearly the same as the error obtained in the conforming finer case.

4.2. An application to the porous media equation with a curved interface. We now consider the advection-diffusion equation with discontinuous porosity ω:

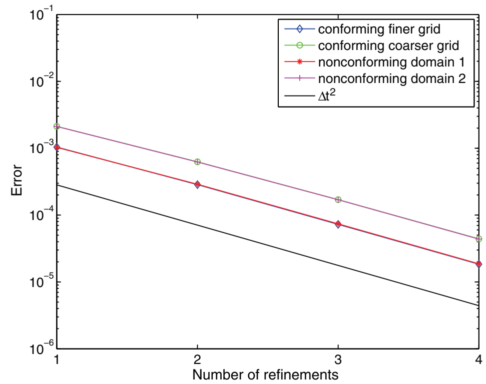

FIG. 4.1. *Error between variational and DG-OSWR solutions versus the refinement in time.*

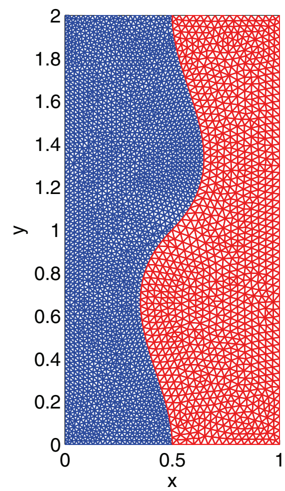

FIG. 4.2. *Domains Ω_1 (left) and Ω_2 (right).*

$$\omega\partial_t u + \nabla\cdot(\boldsymbol{b}u - \nu\nabla u) = 0.$$

The physical domain is $\Omega = (0,1)\times(0,2)$, and the final time is $T = 1.5$. Ω is split into two subdomains. The interface Γ is parametrized with a Hermite polynomial $(\frac{1}{2} + ((2s-1)^3 + 2(2s-1)^2 + (2s-1))\mathbb{1}_{s\le\frac{1}{2}} + ((2s-1)^3 - 2(2s-1)^2 + (2s-1))\mathbb{1}_{s\ge\frac{1}{2}})$ for $0 < s < 1$; see Figure 4.2. The advection, diffusion, and porosity coefficients are $\boldsymbol{b}_1 = (-\sin(\frac{\pi}{2}(y-1))\cos(\pi(x-\frac{1}{2})), 3\cos(\frac{\pi}{2}(y-1))\sin(\pi(x-\frac{1}{2})))$, $\nu_1 = 0.003$, $\omega_1 = 0.1$, $\boldsymbol{b}_2 = \boldsymbol{b}_1$, $\nu_2 = 0.01$, and $\omega_2 = 1$.

We analyze in Figure 4.3 the precision versus the time step. The process is stopped when the residual is smaller than 10^{-12}. A variational reference solution is computed on a time grid with 7680 time steps. The nonconforming in time solutions are interpolated on the previous grid to compute the error. We start with a time grid with 120 time steps for the left domain and 26 time steps for the right domain and divide the time steps by 2 several times. Figure 4.3 shows the norms of the error in $L^\infty(I, L^2(\Omega_i))$ versus the time steps for both subdomains. We observe the order 2 in time for the nonconforming case. In Figure 4.3 we show also the norms of the error in $L^2(\Omega_i)$ at final time $t = T$ versus the time steps for both subdomains. The error is of superconvergent order as in [24].

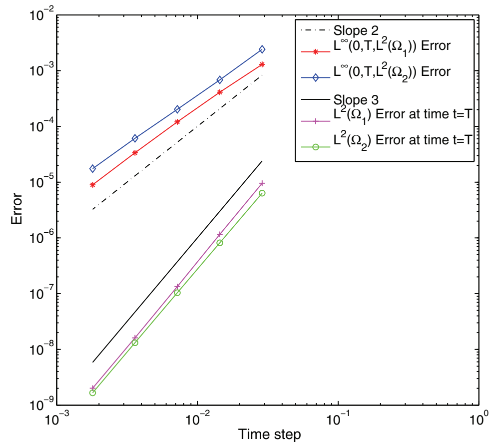

FIG. 4.3. *Error curves versus the refinement in time.*

4.3. Complexity issue, an example of ocean-atmosphere coupling. The motivation for using nonconforming space-time grids is primarily to adapt the mesh to the underlying model, permitting fast and independent solvers in the subdomains, and to be able to couple different codes with different resolutions, and even different models.

As a first step toward ocean-atmosphere coupling, the following model was introduced by Blayo and Lemarié within the ANR project COMMA [20].

4.3.1. Definition of the model. The evolution of salt tracers is represented by a bidimensional advection-diffusion equation with anisotropic diffusion (z is the vertical coordinate):

$$\frac{\partial u}{\partial t} + \nabla \cdot (\boldsymbol{a}(x,z)u - D(z)\nabla u) = 0.$$

The ocean is the domain $(0, L) \times (-h_O, 0)$, and the atmosphere is the domain $(0, L) \times (0, h_A)$ with $h_O = 5km$, $h_A = 30km$, and $L = 5000km$. The velocity field and diffusion tensor are

$$\vec{a}(x,z) = \begin{cases} (\frac{50}{6}\sin(\frac{2\pi x}{L})\cos(\frac{\pi z}{h_A}), -0.1\cos(\frac{2\pi x}{L})\sin(\frac{\pi z}{h_A})), & -h_O \le z \le 0, \\ (0.5\sin(\frac{2\pi x}{L})\cos(\frac{\pi z}{h_O}), -0.001\cos(\frac{2\pi x}{L})\sin(\frac{\pi z}{h_O})), & 0 \le z \le h_A, \end{cases}$$

$$D(z) = \begin{pmatrix} \nu_x(z) & 0 \\ 0 & \nu_z(z) \end{pmatrix},$$

with

$$\nu_x = \begin{cases} 100, & z \le 0, \\ 10000, & z \ge 0, \end{cases} \quad \nu_z(z) = \begin{cases} 10^{-5} + (10^{-2} - 10^{-5})e^{\frac{-(z+100)^2}{8000}}, & z \le 0, \\ 10^{-3} + (0.1 - 10^{-3})e^{\frac{-(z-30)^2}{1000}}, & z \ge 0. \end{cases}$$

The initial state is

$$u_0 = \begin{cases} 14e^{(-\frac{ln(7)}{10^5}(z+495)^2)} + 2, & -h_O \le z \le -495, \\ 16, & -495 \le z \le 0, \\ 16 - \frac{41z}{30000}, & 0 \le z \le h_A. \end{cases}$$

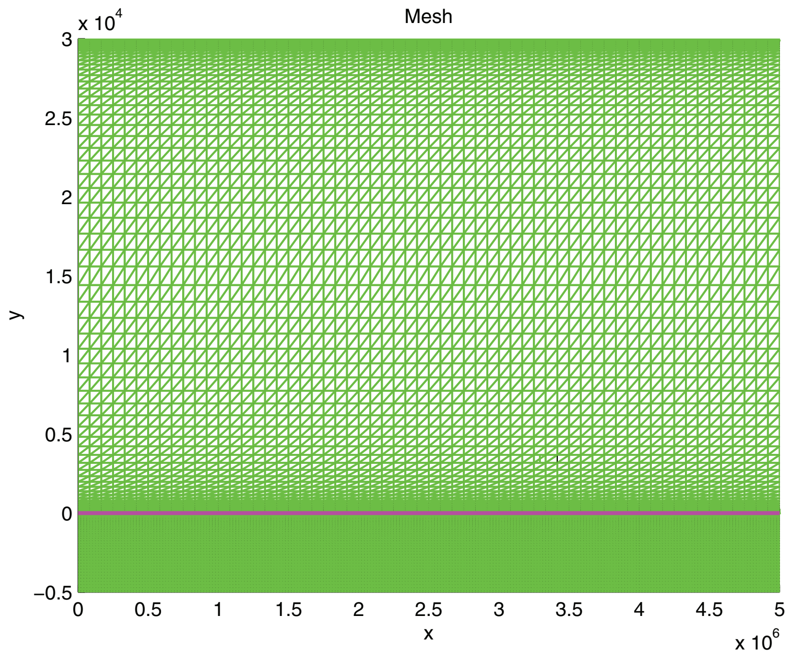

Fig. 4.4. *Mesh.*

The total time of computation is five days. Homogeneous Neumann boundary conditions are enforced on all exterior boundaries.

4.3.2. Definition of the grid. The spatial grid is made of rectangles, each of them divided into two triangles. The rectangular grid is uniform in the x direction with $N_{A,x} = 60$ points in the atmosphere and $N_{O,x} = 240$ points in the ocean. The vertical grid in z is nonlinear (to increase the resolution near the surface; see Figure 4.4), with $N_{A,z} = 70$ grid points in the atmosphere and $N_{O,z} = 50$ grid points in the ocean. The computation is divided into $N_w = 20$ time windows of six hours each. In each time window different time steps are used in the two domains: $N_{A,t} = 90$ points in the atmosphere and $N_{O,t} = 12$ points in the ocean. This corresponds to realistic measurement intervals.

4.3.3. Computation. The monodomain solution is computed on the finer grid in time and space, i.e., with $N_x = \max(N_{0,x}, N_{A,x}) = 240$, $N_z = N_{O,z} + N_{A,z} = 120$, and $N_t = \max(N_{O,t}, N_{A,t}) = 90$. For each computation, whether local or global, a linear system must be solved at each time step. Its size is the total number of points in space. A direct method is used, the LU decomposition is performed once and for all in each subdomain, and only lower order operations are made in the iteration loop. Furthermore the LU decompositions in the subdomains are computed in parallel. The space-time nonconforming DG-OSWR solution is computed with $k = 3$ iterations per time window. In each window, the initial guess is computed by applying the Venctell operator to a solution constant in time, equal to the computed solution at the final time of the previous window (or equal to the initial condition for the first window).

In Figure 4.5, we observe the DG-OSWR multidomain solution. In Table 4.1 we observe the relative $L^\infty(0, T; L^2(\Omega_i))$ errors in the ocean and in the atmosphere versus the iterations. A comparison is given in the last column with the converged solution,

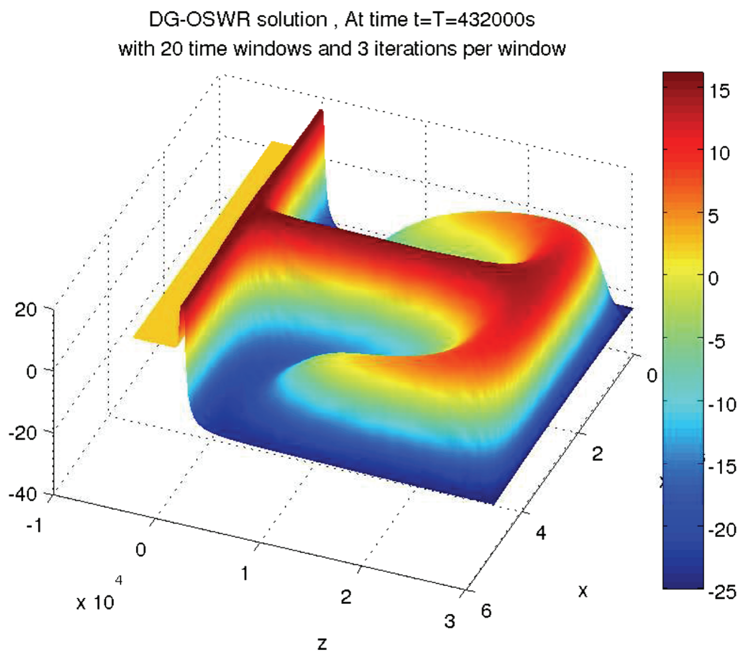

FIG. 4.5. *DG-OSWR solution at final time $T = 5$ days.*

TABLE 4.1
Relative $L^2(\Omega_i \times (0,T))$ errors versus the iterations. The converged solution is computed with a residual smaller than 10^{-12} in each time window. The last two lines are the relative L^2 error in time and space for the 15th first grid levels close to the surface.

L^2 relative error	$k = 1$	$k = 2$	$k = 3$	Converged
ocean	6.129e-03	6.946e-04	6.815e-04	6.815e-04
atmosphere	3.442e-03	3.354e-03	3.354e-03	3.354e-03
ocean (close to the surface)	4.904e-03	5.062e-04	4.977e-04	4.976e-04
atmosphere (close to the surface)	8.685e-04	4.659e-04	4.659e-04	4.659e-04

computed with a residual smaller than 10^{-12} in each time window. We remark that iterating further $k = 3$ in the subdomains does not modify the errors; therefore, three iterations per time window are sufficient to reach the global scheme accuracy.

4.3.4. Comparison with the classical Schwarz waveform relaxation. For comparison, we introduce the overlapping algorithm with Dirichlet transmission conditions (referred to in what follows as the "classical" algorithm). Note that Dirichlet conditions in the nonoverlapping case do not lead to a convergent algorithm [4]. We consider two cases: $L = 1$ meter, which corresponds to an overlap of one node, and $L = 80$ meters, which corresponds to an overlap of six nodes in z. We consider one time window of five days. We impose a random initial guess on the space-time interface and perform the algorithm using various transmission conditions: Dirichlet in the overlapping case and optimized Ventcell conditions in the nonoverlapping case.

In Figure 4.6 we plot the relative L^2 error with the global monodomain solution versus the number of iterations, for conforming grids in time and space on the interface. One can see that the overlapping Schwarz algorithm using Dirichlet conditions converges very slowly while the use of optimized Ventcel conditions without overlap

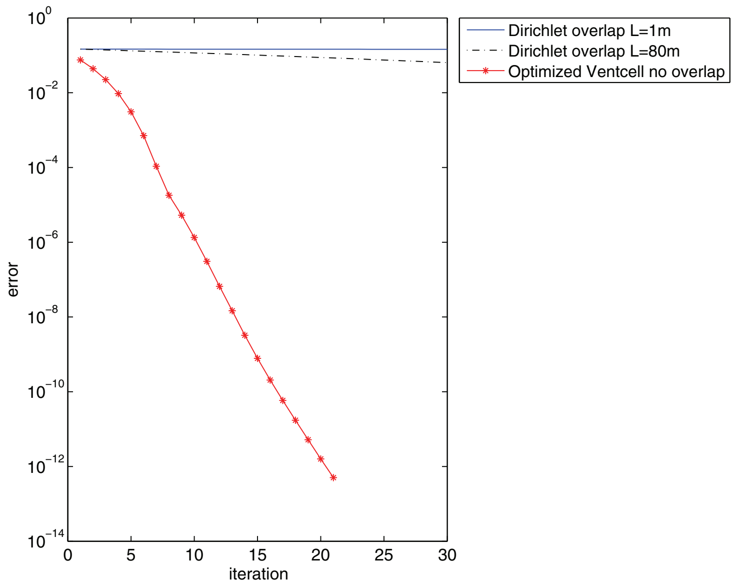

FIG. 4.6. *Error versus iterations of the domain decomposition iterates.*

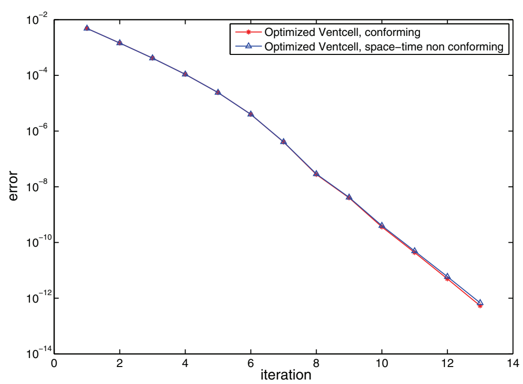

FIG. 4.7. *Error versus iterations for conforming and space-time nonconforming grids.*

let the algorithm converge much faster. In Figure 4.7 we plot the error versus the number of iterations for conforming grids (star line) and space-time nonconforming grids (triangle line). In this case, the initial guess is computed from the initial condition (by applying the Venctell operator to a solution constant in time, equal to the initial condition at each time step). We observe that using nonconforming grids in time and in space does not affect the convergence speed of the algorithm.

4.3.5. Theoretical comparison of the computational costs. We finally compare the computational costs (complexity, i.e., number of elementary operations) of the monodomain and the multidomain algorithms. We introduce the following notation:

- N_1 is the number of elementary operations used for the computation of the monodomain solution.
- $N_2(k)$ is the number of elementary operations used in the Schwarz waveform relaxation algorithm with k iterations.

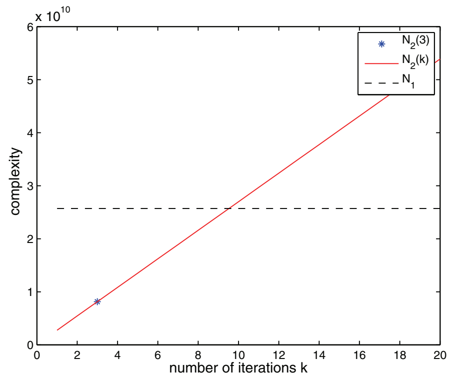

FIG. 4.8. *Complexity: Comparison of full fine computation/domain decomposition and nonconforming mesh refinement.*

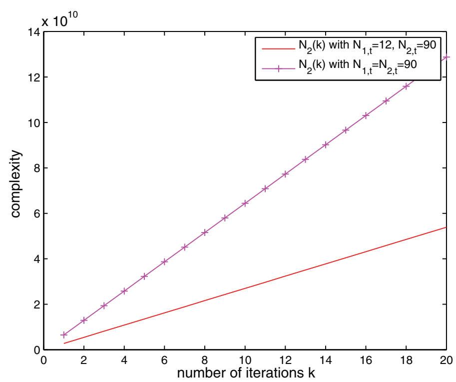

FIG. 4.9. *Complexity: Comparison of conforming/nonconforming grids in time.*

Recall that if an $n\times n$ matrix A has bandwidth n_b, then the LU factorization algorithm involves about $2n\,n_b^2$ operations (see [8]), while each triangular resolution requires about $2n\,n_b$ operations. In the computation here, the number of triangles is such that $n_b = N_z$. Then, the complexities can be expressed as

(4.1)

$$\begin{aligned} N_1 &\sim 2N_z^3 N_x + 4N_z^2 N_x N_t N_w, \\ N_2(k) &\sim 2\max(N_{A,z}^3 N_{A,x}, N_{O,z}^3 N_{O,x}) + 4k\max(N_{A,z}^2 N_{A,x} N_{A,t} + N_{O,z}^2 N_{O,x} N_{O,t}) N_w. \end{aligned}$$

Figures 4.8 and 4.9 illustrate the complexities of the methods with numerical data from our example. Figure 4.8 represents $N_2(k)$ and N_1 versus the number of iterations p. We see that the domain decomposition algorithm is cheaper if the number of iterations is smaller than 12. The star on the picture is set at $k = 3$, which is the number of necessary iterations. The gain is important, since

$$\text{theoretical speed-up } = \frac{N_1}{N_2(3)} = 3.1594.$$

We furthermore compare in Figure 4.9 the complexity when using domain decomposition with nonconforming grids in time as above (solid line) or conforming grids in time with the smallest time step (plus-solid line), keeping nonconforming grids in space. In the latter case, the speed-up, computed with formulas (4.1), is about 2 for $k = 3$.

4.3.6. Numerical estimation of the computational costs. These theoretical results fit with the cpu time and elapsed time that are measured in the computations with MATLAB:

$$\text{Numerical speed-up } = \begin{cases} 3.0203e+00 \text{ measured by the cputime function,} \\ 2.9281e+00 \text{ measured by the tic and toc functions.} \end{cases}$$

5. Conclusion. We have proposed a new numerical method to solve parabolic equations with discontinuous coefficients and curved interfaces. It relies on the splitting of the time interval into time windows, in which a few iterations of an optimized Schwarz waveform relaxation algorithm are performed by a discontinuous Galerkin method in time, with nonconforming projection between space-time grids on the interfaces. We have shown numerically that the method preserves the order of the discontinuous Galerkin method. The nonconforming domain decomposition method permits us to couple heterogeneous models with different resolutions adapted to the physics with a significant gain in computation time (about a factor 3 in our example) compared with the classical method with a conforming space-time grid in all the subdomains. A fully discrete scheme (with new mortar elements) will be presented and analyzed in a further work.

REFERENCES

[1] D. Bennequin, M. J. Gander, and L. Halpern, *A homographic best approximation problem with application to optimized Schwarz waveform relaxation*, Math. Comp., 78 (2009), pp. 185–223.

[2] E. Blayo, L. Halpern, and C. Japhet, *Optimized Schwarz waveform relaxation algorithms with nonconforming time discretization for coupling convection-diffusion problems with discontinuous coefficients*, in Decomposition Methods in Science and Engineering XVI, O. B. Widlund and D. E. Keyes, eds., Lect. Notes Comput. Sci. Eng. 55, Springer, Berlin, 2007, pp. 267–274.

[3] M. J. Gander, L. Halpern, and F. Nataf, *Optimal convergence for overlapping and non-overlapping Schwarz waveform relaxation*, in Proceedings of the 11th International Conference of Domain Decomposition Methods C. H. Lai et al., eds., Greenwich, England, 1999, available online from http://www.ddm.org/DD11/index.html.

[4] M. J. Gander and L. Halpern, *Optimized Schwarz waveform relaxation methods for advection reaction diffusion problems*, SIAM J. Numer. Anal., 45 (2007), pp. 666–697.

[5] M. J. Gander, L. Halpern, and M. Kern, *Schwarz waveform relaxation method for advection–diffusion–reaction problems with discontinuous coefficients and non-matching grids*, in Decomposition Methods in Science and Engineering XVI, O. B. Widlund and D. E. Keyes, eds., Lect. Notes Comput. Sci. Eng. 55, Springer, Berlin, 2007, pp. 916–920.

[6] M. J. Gander, C. Japhet, Y. Maday, and F. Nataf, *A new cement to glue nonconforming grids with Robin interface conditions: The finite element case*, in Domain Decomposition Methods in Science and Engineering, R. Kornhuber et al., eds., Lect. Notes Comput. Sci. Eng. 40, Springer, Berlin, 2005, pp. 259–266.

[7] F. Gastaldi, L. Gastaldi, and A. Quarteroni, *Adaptive domain decomposition methods for advection dominated equations*, East-West J. Numer. Math., 4 (1996), pp. 165–206.

[8] G. Golub and C. V. Loan, *Matrix Computations*, The John Hopkins University Press, Baltimore, MD, 1989.

[9] L. Halpern and C. Japhet, *Discontinuous Galerkin and nonconforming in time optimized Schwarz waveform relaxation for heterogeneous problems*, in Decomposition Methods in Science and Engineering XVII, U Langer et al., eds., Lect. Notes Comput. Sci. Eng. 60, Springer, Berlin, 2008, pp. 211–219.

[10] L. Halpern, C. Japhet, and P. Omnes, *Nonconforming in time domain decomposition method for porous media applications*, in the 5th European Conference on Computational Fluid Dynamics ECCOMAS CFD, J. C. F. Pereira and A. Sequeira, eds., Lisbon, Portugal, 2010.

[11] L. Halpern, C. Japhet, and J. Szeftel, *Discontinuous Galerkin and nonconforming in time optimized Schwarz waveform relaxation*, in Domain Decomposition Methods in Science and Engineering XIX, Lect. Notes Comput. Sci. Eng., Springer, Berlin, 2010, pp. 133–140; also available online from http://numerik.mi.fu-berlin.de/DDM/DD18/.

[12] L. Halpern, C. Japhet, and J. Szeftel, *Space-time nonconforming optimized Schwarz waveform relaxation for heterogeneous problems and general geometries*, in Domain Decomposition Methods in Science and Engineering XIX, Lect. Notes Comput. Sci. Eng., Springer, Berlin, 2010, pp. 75–86.

[13] C. Japhet, *Méthode de décomposition de domaine et conditions aux limites artificielles en mécanique des fluides: Méthode Optimisée d'Ordre* 2 *(OO*2*)*, Ph.D. thesis, Université Paris 13, Paris, France, 1998.

[14] C. Japhet, *Optimized Krylov-Ventcell method. Application to convection-diffusion problems*, in Proceedings of the 9th International Conference on Domain Decomposition Methods, P. E. Bjorstal et al., eds., Bergen, Norway, 1998, pp. 382–389.

[15] C. Johnson, K. Eriksson, and V. Thomee, *Time discretization of parabolic problems by the discontinuous Galerkin method*, RAIRO Modél. Math. Anal. Numér., 19 (1985), pp. 611–643.

[16] J.-L. Lions and E. Magenes, *Problèmes aux limites non homogènes et applications*, Travaux et Recherches Mathématiques 18, Dunod, Paris, 1968.

[17] C. Makridakis and R. Nochetto, *A posteriori error analysis for higher order dissipative methods for evolution problems*, Numer. Math., 104 (2006), pp. 489-514.

[18] V. Martin, *An optimized Schwarz waveform relaxation method for unsteady convection diffusion equation*, Appl. Numer. Math., 52 (2005), pp. 401–428.

[19] F. Nataf and F. Rogier, *Factorization of the convection-diffusion operator and the Schwarz algorithm*, M^3AS, 5 (1995), pp. 67–93.

[20] ANR project COMMA, *Coupling in Multi-physics and Multi-scale Problems: Models and Algorithms*, available online from http://comma-ljk.imag.fr.

[21] B. Sheehan, D. Estep, S. Tavener, J. Cary, S. Kruger, A. Hakim, A. Pletzer, J. Carlsson, and S. Vadlamani, *The Interaction of Iteration Error and Stability for Time Dependent Linear* PDE*'s coupled through an Interface*, Technical report, University of Colorado, 2011.

[22] J. Szeftel, *Absorbing boundary conditions for reaction-diffusion equations*, IMA J. Appl. Math., 68 (2003), pp. 167–184.

[23] J. Szeftel, *Calcul pseudo-différentiel et para-différentiel pour l'étude des conditions aux limites absorbantes et des propriétés qualitatives des EDP non linéaires*, Ph.D. thesis, Université Paris 13, Paris, France, 2004.

[24] V. Thomee, *Galerkin Finite Element Methods for Parabolic Problems*, Springer, Berlin, 1997.